RIMS-1988

Anyon Condensation in Virasoro TQFT: Wormhole Factorization

By

Shunta TAKAHASHI

December 2024

京都大学　数理解析研究所

Anyon Condensation in Virasoro TQFT: Wormhole Factorization

Shunta Takahashi

Research Institute for Mathematical Science (RIMS), Kyoto University, Kyoto 606-8502, Japan

E-mail: shunta@kurims.kyoto-u.ac.jp

ABSTRACT: Anyon condensation in wormhole geometries is investigated in the Virasoro TQFT (VTQFT) formulation. We first review some elementary techniques of VTQFT and verify its consistency by showing that it reproduces semiclassical results, including the Hawking-Page phase transition and the Bekenstein-Hawking entropy of BTZ blackhole. We then summarize a gauging scheme for non-invertible symmetries referred to as anyon condensation and exhibit that it is applicable to VTQFT even though the category of Wilson lines associated with it is not strictly a modular tensor category (MTC). More specifically, it is shown that the partition function of the wormhole factorizes upon condensating the so-called diagonal condensable anyon in VTQFT.

KEYWORDS: 3d quantum gravity, Virasoro TQFT, anyon condensation

Contents

1 Introduction

Seeking well-defined quantum gravity is essential for advancing our understanding of fundamental physics. In three-dimensional spacetime, the gravitational dynamics are significantly simplified compared to higher dimensions, providing a tractable model for studying quantum gravitational effects. Indeed, Ref. [1] establishes a direct connection between 3d Einstein-Hilbert action with negative cosmological constant and $SL(2,\mathbb{R}) \times SL(2,\mathbb{R})$ Chern-Simons action, showing that the $\mathfrak{sl}(2,\mathbb{R}) \times \mathfrak{sl}(2,\mathbb{R})$ gauge fields A_μ and $\overline{A}_\mu$ are expressed in terms of the dreibein e_μ^a and the spin connection ω_μ^a as

$$A_\mu^a = e_\mu^a + \frac{i}{l}\omega_\mu^a, \quad \overline{A}_\mu^a = e_\mu^a - \frac{i}{l}\omega_\mu^a, \tag{1.1}$$

which ensures that 3d gravity is topological at the classical level in a sense that it does not depend on the spacetime metric, as Chern-Simons action is manifestly topological. The quantization of Chern-Simons theory yields a topological quantum field theory (TQFT) described by the conformal blocks of Wess-Zumino-Witten (WZW) model that resides on the boundaries [2]. However, there is a subtlety as the generic path-integral quantization scheme implements the integral over all configurations of dynamical fields (variables of path-integral) A_μ^a in Chern-Simons theory that may result in a non-invertible dreibein e_μ^a. In

quantum gravity, the gravitational path integral $Z_{\text{gravity}} = \int \mathcal{D}g_{\mu\nu}\, S_{\text{gravity}}[g_{\mu\nu}]$ is performed over geometries $g_{\mu\nu} = e_\mu^a e_\nu^b \eta_{ab}$ which are supposed to be non-degenerate. Consequently, while Chern-Simons theory offers valueable insights, it serves as a preliminary toy model rather than a complete framework for the development of quantum gravity.

In order to circumvent such a conundrum, one should select the so-called Teichmüller component from the classical phase space of Chern-Simons thoery and quantize the space of holomorphic sections of a certain line bundle over it [3]. Seminal work by H. Verlinde [4] addresses this quantization issue and reveals that the resulting Hilbert space is a collection of Virasoro conformal blocks of Liouville theory equipped with an abstract inner product (2.1). This statement is refined by J. Teschner in his series of works [5–8] and has been investigated extensively in mathematics literatures [9–11]. Recent work by S. Collier et al. [12, 13] advocated more tractable form of the impractical inner poduct (2.1), whose explicit expression is provided in Subsection 2.1. They renamed the conventional Teichmüller-based TQFT with the new inner product as *Virasoro TQFT* (VTQFT), for the Hilbert space associated with the 2d boundaries is a collection of Virasoro conformal blocks. Building on their formalism, the qunatum gravity partition function is given for any 3d hyperbolic geometry M as

$$Z_{\text{gravity}}(M) = \sum_{\gamma \in \text{MCG}(\partial M)/\text{MCG}(M)} |Z_{\text{Vir}}(\gamma \cdot M)|^2, \tag{1.2}$$

even when it is uncertain whether the conventional metric approach for path-integral is readily applicable. $\text{MCG}(M) := \text{Diff}(M)/\text{Diff}_0(M) \cong \pi_0(\text{Diff}(M))$ is the mapping class group of the 3-manifold M.[1] Notably, this rule successfully reproduces the Maloney-Witten sum for solid torus geometries [14]. Another way to support its credibility is to compare the partition function to that of a putative holographic dual 2d CFT which has been the focus of intensive investigation in recent years [15–19]. In the literature, it is strongly suggested that the dual CFT is not a particular pure CFT but rather one characterized by a Gaussian ensemble average of observables supplimented with non-Gaussian corrections. However, this leads to a significant enigma known as the *factorization puzzle*, which involves the non-factorization of the partition function for geometries with multiple boundaries.

A potential solution to that puzzle emerges from another paradigm referred to as *generalized global symmetries* [20]. In this framework, the notion of "symmetries" is reinterpreted as invariance under the action of higher-dimensional topological operators. Of particular relevance to our present discussion are *non-invertible symmetries* [21, 22], forming a symmetry category rather than a symmetry group due to the absence of inverse operations. Non-Abelian TQFTs provide typical examples, with their Wilson lines serving as simple objects in symmetry categories possibly with non-trivial fusion rule $L_i \otimes L_j = \bigoplus_k N_{ij}^k L_k$ ($\sum_k N_{ij}^k > 1$). For 3d TQFT, the associated category is a *modular tensor category* (MTC), roughly described as a fusion category with a braiding structure. Anyon condensation is a non-invertible version of gauging 1-form symmetry and similar to the invertible case, this process requires selecting a "'t Hooft anomaly-free" object, or a *condensable anyon*, from the MTC. Mathematically, such an object is a connected commutative separable Frobenius algebra object in a braided monoidal category. In Ref. [23] it is shown that the anyon condensation for a general condensable anyon in non-Abelian Chern-Simons theory leads to partition function factrization in two-boundary wormhole geometry

---

[1]Since a homeomorphism sends the boundary to the boundary, a bulk diffeomorphim f induces the boundary diffeomorphism $f|_{\partial M}$, for which we can regard $\text{MCG}(M)$ as a subset of $\text{MCG}(\partial M)$.

as one would expect given that global symmetries are absent in a bulk quantum gravity theory with a CFT dual [24, 25]. The approach should also be feasible within VTQFT as pointed out in Refs. [12, 26], and we show that the factorization indeed manifests in the two-boundary wormhole geometry when we consider the *diagonal Lagrangian condensable anyon* despite the fact that their symmetry category is not a MTC, much less a tensor category, due to the continuum of lines. We obtain a meaningful result partly because VTQFT retains a well-behaved braiding structure.

This paper is organized as follows. In Section 2, we briefly review the foundation of Virasoro TQFT and show that the semiclassical phenomena like Hawking-Page transition and Bekenstein-Hawking entropy can be derived within this framework. Section 3 introduces general gauging method for non-Abelian TQFTs known as anyon condensation. We itemize various conditions for an object in symmetry category $\mathcal{C}$ to be gaugeable and define diagonal Lagrangian algebra object in the special case of $\mathcal{C} \boxtimes \overline{\mathcal{C}}$. Section 4 is devoted to the presentation of the main result. We establish a crucial relation involving an elementary bulding block called the projector, and then go on to prove that the partition function of two-boundary wormhole factorizes veritably by virtue of anyon condensation. Section 5 provides concluding remarks on our result and future directions. Appendix A encapsulates numerous consistency equations for crossing transformations of Virasoro conformal blocks that are ubiquitous throughout the main body. They are essentially a consequence of the non-rational version of the Moore-Seiberg consistency conditions. In Appendix B, we re-cap several core categorical terms needed to formulate fusion category and modular tensor category. The interrelations among them are visualized in a diagram which may also assist readers in consulting other relevant literature.

2   Virasoro TQFT

In this section, we provide an outline of Virasoro TQFT [12] to put it into practice in Section 4. We begin by reviewing the Hilbert space structure and the action of crossing transformations in Subsection 2.1, followed by a summary of the VTQFT path-integral rule in Subsection 2.2. In Subsection 2.3, we provide a justification for VTQFT as a 3d gravitational theory by reproducing the Hawking-Page phase transition in 3d and the Bekenstein-Hawking entropy of the BTZ blackhole. Before proceeding, let us briefly explore the interplay between the theory and Chern-Simons theory, as well as the pivotal role of the quantization of Teichmüller space.

Suppose the spacetime manifold is of the form $\Sigma \times \mathbb{R}$, where Σ is a closed Riemann surface. As established in Ref. [3], the classical phase space of $SL(2, \mathbb{R})$ Chern-Simons theory on $\Sigma \times \mathbb{R}$ is the moduli space $\mathcal{M}_{\text{flat}}$ of flat $SL(2, \mathbb{R})$-bundles (principal $SL(2, \mathbb{R})$-bundles equipped with flat connections) over Σ. This arises because the EOMs from the Chern-Simons action require that the curvature be vanishing. In bundle theory [27], each flat $SL(2, \mathbb{R})$-bundle, combined with the 2d fundamental representation of $SL(2, \mathbb{R})$, induces the associated vector bundle of rank 2. The Euler number of this bundle takes a specific value from $-(2g-2), -(2g-3), \cdots, 2g-3$, or $2g-2$, where the upper bound $2g-2$ coincides with the Euler number $\chi(\Sigma)$ of the tangent bundle $T\Sigma$. All the flat $SL(2, \mathbb{R})$-bundles are classified according to the Euler number of their associated bundles ranging from $-(2g-2)$ to $2g-2$. The moduli space $\mathcal{M}_{\text{flat}}$ has indeed $(2g-2)-(-(2g-2))+1 = 4g-3$ connected components labeled by the Euler number. On the other hand, there is a one-to-one correspondence between flat $SL(2, \mathbb{R})$-bundles and holonomy representations ρ :

$\pi_1(\Sigma) \to SL(2, \mathbb{R})$ which may or may not be continuous. There is another match between *discrete* embeddings $\pi_1(\Sigma) \to SL(2, \mathbb{R})$ and complex structures of Σ, so only a limited class of flat $SL(2, \mathbb{R})$-bundles defines complex structures on Σ. All other flat bundles result in singular geometries which are unfavorable in gravity theory. Notably, the flat bundles in that class happen to be exactly those within the single connected component of $\mathcal{M}_{\text{flat}}$ with maximal Euler number $2g-2$. This component is isomorphic to the ***Teichmüller space*** $\mathcal{T}_\Sigma$ of Σ, the universal covering space of moduli space $\mathcal{M}_\Sigma$ of Σ related by $\mathcal{M}_\Sigma = \mathcal{T}_\Sigma / \text{MCG}(\Sigma)$ where MCG is the mapping class group [28]. Thus, the quantization of 3d gravity with a negative cosmological constant reduces to the quantization of Teichmüller space. These deductions are heavily reliant on the mathematical results by M. F. Atiyah and R. Bott [29].

As noted earlier the quantization of the Teichmüller space associated with the n-punctured genus g Riemann surface $\Sigma_{g,n}$ gives rise to a Hilbert space $\mathcal{H}_{g,n}$ whose elements are Virasoro conformal blocks $\big|\mathcal{F}_{g,n}^{\mathcal{C}}(\boldsymbol{p}; \boldsymbol{p}_e)\big\rangle$ of Liouville theory with an abstract inner product [4]

$$\big\langle \mathcal{F}_{g,n}^{\mathcal{C}}(\boldsymbol{p}; \boldsymbol{p}_e) \big| \mathcal{F}_{g,n}^{\mathcal{C}}(\boldsymbol{p}'; \boldsymbol{p}_e) \big\rangle = \int_{\mathcal{T}_{g,n}} d^{6g-6+2n}\boldsymbol{m}\; Z_{bc} Z_{\text{TLL}} \overline{\mathcal{F}_{g,n}^{\mathcal{C}}(\boldsymbol{p}; \boldsymbol{p}_e | \boldsymbol{m})} \mathcal{F}_{g,n}^{\mathcal{C}}(\boldsymbol{p}'; \boldsymbol{p}_e | \boldsymbol{m}), \quad (2.1)$$

where $\boldsymbol{p} \in \mathbb{R}_{\geq 0}^{3g-3+n}$ (resp. $\boldsymbol{p}_e \in \mathbb{R}_{\geq 0}^{n}$) is an internal (resp. external) Liouville momenta w. r. t. a conformal block decomposition channel $\mathcal{C}$ and $\boldsymbol{m}$ is the moduli coordinates on the Teichmüller space $\mathcal{T}_{g,n}$. Z_{bc} is the bc ghost partition function for gauge fixing and Z_{TLL} is the timelike Liouville partition function to cancel the Weyl anomaly just as in string theory. The holomorphic conformal block functions $\mathcal{F}_{g,n}^{\mathcal{C}}(\boldsymbol{p}; \boldsymbol{p}_e; \boldsymbol{m})$ are obtained by taking overlap between the moduli basis $|\boldsymbol{m}\rangle$ ($\boldsymbol{m} \in \mathcal{T}_{g,n}$) and the conformal block basis $\big|\mathcal{F}_{g,n}^{\mathcal{C}}(\boldsymbol{p}; \boldsymbol{p}_e)\big\rangle$

$$\mathcal{F}_{g,n}^{\mathcal{C}}(\boldsymbol{p}; \boldsymbol{p}_e; \boldsymbol{m}) := \big\langle \boldsymbol{m} \big| \mathcal{F}_{g,n}^{\mathcal{C}}(\boldsymbol{p}; \boldsymbol{p}_e) \big\rangle. \quad (2.2)$$

In gravitational theory, we need to consider the product of the chiral and the anti-chiral sector to determine the partition function (1.2). Hence the classical phase space of gravity is $\mathcal{T}_{g,n} \times \overline{\mathcal{T}}_{g,n}$ [30], where $\overline{\mathcal{T}}_{g,n}$ is the orientation reversal of $\mathcal{T}_{g,n}$. We will next explore the Hilbert space structure in detail. We only describe the chiral part $\mathcal{T}_{g,n}$ for simplicity, but the same goes for the anti-chiral part unless stated otherwise.

2.1 The Hilbert space and the crossing transformations

As we see above the Hilbert space $\mathcal{H}_{g,n}$ associated with a Riemann surface $\Sigma_{g,n}$, possibly with punctures, is the space of Virasoro conformal blocks on $\Sigma_{g,n}$. They are parametrized by basic CFT data, namely the central charge and the spectrum (the conformal weights of the operator contents).

The Liouville parameter b is related to the Chern-Simons level k as

$$b = \frac{1}{\sqrt{k-2}} = \frac{1}{\sqrt{\frac{l}{4G} - 2}}, \quad (2.3)$$

where l is the AdS radius and G is the 3d Newton constant. In terms of the back ground charge $Q := b + \frac{1}{b}$ the central charge takes the form

$$c = 1 + 6Q^2 = 13 + 6b^2 + \frac{6}{b^2} = 1 + \frac{3l}{2G} + \frac{6}{\frac{l}{4G} - 2}, \quad (2.4)$$

which asymptotes to the Brown-Henneaux value $c = \frac{3l}{2G}$ in the semiclassical limit $G \to 0$. The conformal weight h_p is parametrized by Liouville momentum p as

$$h_p = \alpha(Q - \alpha) = \frac{Q^2}{4} + p^2 = \frac{c-1}{24} + p^2 \qquad \left(\alpha := \frac{Q}{2} + ip \right). \tag{2.5}$$

The state with the conformal weight h_p is normalizable only when $p \in \mathbb{R}_{\geq 0}$ or equivalently when h_p is above the threshold $\frac{c-1}{24}$, and it is noteworthy that the identity line $\mathbb{1}$ ($h_{\mathbb{1}} = 0$) is unnormalizable whose Liouville momentum is $p = \pm i\frac{Q}{2}$. We will frequently express $p \to \mathbb{1}$ instead of $p = \pm i\frac{Q}{2}$ to clarify that the Wilson line p is mapped to the identity line $\mathbb{1}$.

In VTQFT, the abstract inner product (2.1) is proposed to have a simplified form[2]

$$\langle \mathcal{F}_{0,3}(\boldsymbol{p}_e) | \mathcal{F}_{0,3}(\boldsymbol{p}_e) \rangle = \frac{1}{C_0(p_1, p_2, p_3)} \qquad \left(\boldsymbol{p}_e = (p_1, p_2, p_3)^T \right), \tag{2.6}$$

$$\langle \mathcal{F}_{g,n}^{\mathcal{C}}(\boldsymbol{p}_1; \boldsymbol{p}_e) | \mathcal{F}_{g,n}^{\mathcal{C}}(\boldsymbol{p}_2; \boldsymbol{p}_e) \rangle = \frac{\delta^{(3g-3+n)}(\boldsymbol{p}_1 - \boldsymbol{p}_2)}{\rho_{g,n}^{\mathcal{C}}(\boldsymbol{p}_1)} \qquad ((g, n) \neq (0, 3)). \tag{2.7}$$

Here, the subscript e attached to the second argument of a conformal block $\mathcal{F}_{g,n}^{\mathcal{C}}$ is the shorthand for "external". The inner product is only defined between blocks with the same external legs. The sphere three-point block ($g = 0, n = 3$) is treated differently since $\dim \mathcal{H}_{0,3} = 1 < \infty$ allows it to be normalizable in the usual sense while any other blocks are only delta-function normalizable due to the fact that $\dim \mathcal{H}_{g,n} = \infty$. The block $|\mathcal{F}_{0,3}(\boldsymbol{p}_e)\rangle$ has the unique channel and no internal momenta, so there are no superscript $\mathcal{C}$ and the only arguments are external Liouville momentum $\boldsymbol{p}_e$. The quantity $\rho_{g,n}^{\mathcal{C}}(\boldsymbol{p}_1)$ in the denominator on the r.h.s. of eq. (2.7) is defined as

$$\rho_{g,n}^{\mathcal{C}}(\boldsymbol{p}) := \prod_{\substack{\text{internal cuffs} \\ a}} \rho_0(p_a) \prod_{\substack{\text{trivalent junctions} \\ (i,j,k)}} C_0(p_i, p_j, p_k), \tag{2.8}$$

where $\rho_0(p_a)$ and $C_0(p_i, p_j, p_k)$ are given by eq. (A.25), (A.13). The "internal cuffs" and the "trivalents junctions" are solely determined by the choice of a channel $\mathcal{C}$ that specifies the way of decomposing the Riemann surface $\Sigma_{g,n}$ into $2g - 2 + n$ pair of pants (3-punctured sphere). There are $2g - 2 + n$ junctions corresponding to each pant and $(3(2g-2+n)-n) \cdot \frac{1}{2} = 3g - 3 + n$ cuffs corresponding to each internal slice. $C_0(p_1, p_2, p_3)$ appears in an universal asymptotic formula for the microcanonical ensemble average of the OPE coefficients of a generic compact unitary 2d CFT with $c > 1$ [32], and is to some extent proportional to the Dorn-Otto-Zamolodchikov-Zamolodchikov (DOZZ) structure constant [33, 34], the sphere

_____

[2]The $\mathcal{N} = 1$ supersymmetric extension is presented in Ref. [31].

3-point coefficient, or equivalently the OPE coefficient, in Liouville theory[3]

$$C_0(p_1, p_2, p_3) \propto \frac{C_{\text{DOZZ}}(p_1, p_2, p_3)}{\sqrt{\prod_{k=1}^{3} S_0(p_k)\rho_0(p_k)}}. \tag{2.11}$$

$C_0(p_1, p_2, p_3)$ is symmetric under exchange of any two arguments due to the symmetricity of $C_{\text{DOZZ}}(p_1, p_2, p_3)$:

$$C_0(p_1, p_2, p_3) = C_0(p_2, p_1, p_3) = C_0(p_3, p_2, p_1). \tag{2.12}$$

Since both $\rho_0(p_a)$ and $C_0(p_i, p_j, p_k)$ are real, the same quantities are employed in computing the inner product in the anti-chiral part. For concreteness, here is an example for the inner product between two 2-punctured torus blocks, where the conformal block $\left|\mathcal{F}_{1,2}^{\mathcal{C}}(p_a, p_b; p_1, p_2)\right\rangle$ is depicted graphically:

$$= \frac{\delta(p_a - p_c)\delta(p_b - p_d)}{\rho_0(p_a)\rho_0(p_b)C_0(p_1, p_a, p_b)C_0(p_2, p_a, p_b)}. \tag{2.13}$$

Intuition behind the inner product (2.7) is the unitarity under the action of the mapping class group $\text{MCG}(\Sigma)$. The image of the projective unitary representation $U_{g,n} : \text{MCG}(\Sigma) \ni \gamma \mapsto U_{g,n}(\gamma) \in \text{End}(\mathcal{H}_{g,n})$ is generated by a non-rational version of basic crossing moves in Moore-Seiberg construction [37] presented below.

(i) fusion transformation

$$= \int_0^{\infty} dp_t \, F_{p_s p_t} \begin{bmatrix} p_1 & p_3 \\ p_2 & p_4 \end{bmatrix} \tag{2.14}$$

(ii) modular S-transformation

$$= \int_0^{\infty} dp' \, S_{pp'}[p_0] \tag{2.15}$$

(iii) braiding

$$= B_{p_3}^{p_1 p_2} \qquad = B_{p_1 p_2}^{p_3} \tag{2.16}$$

---

[3]The explicit factor of proportianality is

$$C_0(p_1, p_2, p_3) = \frac{\left(\pi\mu\gamma(b^2)b^{2-2b^2}\right)^{\frac{Q}{2b}}}{2^{\frac{3}{4}}\pi} \frac{\Gamma_b(2Q)}{\Gamma_b(Q)} \frac{C_{\text{DOZZ}}(p_1, p_2, p_3)}{\sqrt{\prod_{k=1}^{3} S_0(p_k)\rho_0(p_k)}}, \tag{2.9}$$

where the wavy line part is independent of p_1, p_2, p_3. $S_0(p)$ is the Liouville reflection coefficient

$$S_0(p) := (\pi\mu\gamma(b^2)b^{2-2b^2})^{-\frac{2ip}{b}} \frac{\Gamma_b(2ip)\Gamma_b(Q - 2ip)}{\Gamma_b(Q + 2ip)\Gamma_b(-2ip)}. \tag{2.10}$$

For a precise definition and properties of the double gamma function $\Gamma_b(x)$, see e.g. Ref. [35, 36].

While the braiding coefficient is just a phase factor

$$B^{p_1 p_2}_{p_3} = e^{\pi i (h_3 - h_1 - h_2)}, \qquad B^{p_3}_{p_1 p_2} = e^{-\pi i (h_3 - h_1 - h_2)}, \qquad (2.17)$$

the fusion kernel F and the modular S-kernel S have complicated forms (A.17), (A.26). However, it is apparent without knowing such intricacy in depth that the fusion kernel F is symmetric under permuting two rows or two columns

$$F_{p_s p_t} \begin{bmatrix} p_1 & p_3 \\ p_2 & p_4 \end{bmatrix} = F_{p_s p_t} \begin{bmatrix} p_3 & p_1 \\ p_4 & p_2 \end{bmatrix} = F_{p_s p_t} \begin{bmatrix} p_2 & p_4 \\ p_1 & p_3 \end{bmatrix}. \qquad (2.18)$$

All crossing kernels here are complex conjugated in calculating the anti-chiral part of VTQFT though the fusion kernel F is unchanged because it is real. See Appendix A for a variety of corssing equations as a result of Moore-Seiberg consistency condition, namely the pentagon, the hexagon among others. The set of equations are frequently referred to in Subsection 2.2 and Section 4.

We now turn to introduce several important formulae that will be employed in the subsequent calculations. At the outset, let us consider the fusion transformation from the s-channel to the u-channel (see also eq. (3.33) in Ref. [13])

$$(2.19)$$

There is an extra phase factor in the integrand compared to fusion transformation from s-channel to t-channel (2.14) due to the overlap of p_2 and p_3. To prove this equation, we apply the fusion transformation, the braiding and the fusion transformation again

$$(2.20)$$

and at last use the hexagon identity (A.8). It can be seen by exactly the same proof, except for the use of the other verion of the hexagon identity (A.9), that a similar formula holds true when p_2 and p_3 are swapped front and back

$$(2.21)$$

We need additional two momentus link identities regarding **Wilson bubule**, **Wilson triangle** and **Verlinde loop**. The first and the last terms are borrowed from in Ref. [38], while the Wilson triangle is our original designation. The Wilson bubble is a line containing a loop and the Wilson triangle is a tiriangle at a trivalent junction as presented in the l. h. s. of the following identities.

$$
\begin{array}{c}
p_1 \!\!\!\!\!\!\!\!\!\!\! \overset{p_2}{\bigcirc} \!\!\!\!\!\!\!\!\!\!\! p_4 \\
_{p_3}
\end{array}
= \frac{\delta(p_1 - p_4)}{\rho_0(p_1)C_0(p_1,p_2,p_3)} \quad \overset{}{\underset{}{\rule{3cm}{0.4pt}}}{}^{p_1} , \tag{2.22}
$$

$$
\begin{array}{c}
\overset{p_1}{\underset{p_u \, p_t}{\triangle}} \\
{}_{p_2 \;\; p_s \;\; p_3}
\end{array}
= \frac{1}{\rho_0(p_1)C_0(p_1,p_t,p_u)} F_{p_s p_1} \begin{bmatrix} p_3 & p_2 \\ p_t & p_u \end{bmatrix} \quad
\begin{array}{c}
{}^{p_1} \\
\underset{p_2 \qquad p_3}{\bigvee}
\end{array} . \tag{2.23}
$$

These are only valid when the loop and the triangle are placed on a contractible cycle in the bulk, i.e. they must not wrap arround any genera of boundary Riemann surfaces. The proof of these equalities requires some laborious calculations concerning a four-boundary wormhole. The intricacies are not vital to our present discussions, so only those interested may refer to the discussion around eq. (3.45) in Ref. [12] and eq. (3.53) in Ref. [13]. The other one is the Verlinde loop, a Wilson loop that encircles a single line as illustrated below

$$
\underset{p}{\overset{p_2}{\rule{1cm}{0.4pt}\, \bigcirc \,\rule{1cm}{0.4pt}}}{}^{p_1}
= \frac{S_{p p_1}[p_2]}{S_{\mathbb{1} p_1}[\mathbb{1}]} \quad
\overset{p_2}{\underset{\;\; p_1}{\rule{2cm}{0.4pt} \!\! | }} . \tag{2.24}
$$

To prove the equality, one apply the general formula (A.28) in Ref. [38] as follows and then resolve the p loop by the Wilson bubble identity (2.22)

$$
\underset{p}{\overset{p_2}{\rule{1cm}{0.4pt}\, \bigcirc_{\mathbb{1}} \,\rule{1cm}{0.4pt}}}{}^{p_1}
= \int_0^\infty dp' \, F_{\mathbb{1} p_2} \begin{bmatrix} p & p \\ p & p \end{bmatrix} \frac{S_{p p_1}[p']}{S_{\mathbb{1} p_1}[\mathbb{1}]} \quad
\begin{array}{c}
{}^{p_2} \\
p \, \overset{\bigcirc}{} \, p \\
{}_{p' \qquad p_1}
\end{array} . \tag{2.25}
$$

2.2 Heegaard splitting and path-integral on compression bodies

We proceed to establish the procedure for computing the state $|Z_{\mathrm{Vir}}(M)\rangle$ for a 3-manifold M with boundaries $\partial M = \bigsqcup_{i=1}^n \Sigma_{g_i, n_i}$. We refer to the state as the **VTQFT partition function** of M. While VTQFT shares significant similarities with standard TQFTs, there are notable differences due to the presence of the continuous spectrum. In fact, $|Z_{\mathrm{Vir}}(M)\rangle$ is a state in $\bigotimes_{i=1}^n \mathcal{H}_{g_i, n_i}$ or in $\mathbb{C}$ when $\partial M = \emptyset$, although typically $\dim \mathcal{H}_{g_i, n_i} = \infty$. The significant challenge is that the surgery is not always valid in VTQFT since the theory is only sensible for *hyperbolic* manifolds. [4] In Chern-Simons TQFT, the partition function of S^3 is computed by starting with $S^1 \times S^2$ containing a single Wilson line wrapping around the non-contractible cycle in the S^1-direction. One then performs

---

[4]This can partly be understood from the fact that non-hyperbolic manifolds cannot be on-shell (a solution to the classical EOM) in AdS$_3$ gravity.

Dehn surgery on the line, leading to the partition function $Z(S^3) = S_{00}$ [2]. However $Z_{\text{Vir}}(S^3)$ is ill-defined since $S_{\mathbb{1}\mathbb{1}}[\mathbb{1}]$ is not defined in VTQFT. Therefore, the VTQFT path-integral can only be implemented for sufficiently complex geometry, specifically those with boundaries $\Sigma_{g,n}$ satisfying $2 - 2g - n < 0$. Although an unpunctured torus does not meet this criterion—and the inner product of $\mathcal{H}_{1,0}$ is not even delta-function normalizable—it is occasionally discussed as an exception at the level of conformal blocks [12, 18].

At this point, the explicit rules are outlined as follows. The first rule applies to a handlebody (a 3-manifold formed by filling the interior of a Riemann surface $\Sigma_{g,n}$) with a network of Wilson lines $\boldsymbol{p}$ inserted along a channel $\mathcal{C}$ but no extra lines

$$|Z_{\text{Vir}}(S\Sigma_{g,n})\rangle := \left|\mathcal{F}_{g,n}^{\mathcal{C}}(\boldsymbol{p})\right\rangle. \tag{2.26}$$

In particular, the VTQFT path-integral prepares $|Z_{\text{Vir}}(S\Sigma_g)\rangle = \left|\mathcal{F}_g^{\mathcal{C}}(\mathbb{1})\right\rangle$ for an unpunctured Riemann surface with no extra Wilson line insertion. For $(g,n) = (1,0)$, the torus zero-point block $|\mathcal{F}_{1,0}(p)\rangle \in \mathcal{H}_{1,0}$, or equivalently a state on a 2d boundary torus of a 3d solid torus with Wilson line p wrapping around its non-contractible (longitudinal) cycle, is nothing but the Virasoro character. As such, we interchangeably denote it as $|\chi_p\rangle = |\mathcal{F}_{1,0}(p)\rangle$ in what follows. For the wormhole geometry $\Sigma_{g,n} \times [0,1]$, the VTQFT path-integral inserts a complete set of state on both boundaries diagonally

$$|Z_{\text{Vir}}(\Sigma_{g,n} \times [0,1])\rangle := \int d^{3g-3+n}\boldsymbol{p} \; \rho_{g,n}^{\mathcal{C}}(\boldsymbol{p}) \left|\mathcal{F}_{g,n}^{\mathcal{C}}(\boldsymbol{p}; \boldsymbol{p}_e)\right\rangle \otimes \left|\mathcal{F}_{g,n}^{\mathcal{C}}(\boldsymbol{p}; \boldsymbol{p}_e)\right\rangle. \tag{2.27}$$

where the explicit form of the integral measure $\rho_{g_i,n_i}^{\mathcal{C}_i}(\boldsymbol{p}_i)$'s is given in eq. (2.8). For a generic manifold M, we employ the **generalized Heegaard splitting** to divide M into a pair of manifolds $C_{g,n}^{(1)}(g_1, n_1; \cdots; g_{m_1}, n_{m_1})$ and $C_{g,n}^{(2)}(h_1, k_1; \cdots; h_{m_2}, k_{m_2})$. Heegaard splitting is a generic scheme for desomposing a manifold into smaller pieces in the theory of 3-manifolds. We compute the VTQFT partition function for each part and glue them together along the splitting surface, applying a twist by the $U_{g,n}(\gamma)$ for some $\gamma \in \text{MCG}(\Sigma_{g,n})$. $C_{g,n}(g_1, n_1; \cdots; g_m, n_m)$ is referred to as a **compression body** whose boundary consists of the "outer" segment $(\partial C_{g,n})^+ = \Sigma_{g,n}$ and the "inner" segment $(\partial C_{g,n})^- = \bigsqcup_{i=1}^m \Sigma_{g_i,n_i}$ (possibly $(\partial C_{g,n})^- = \emptyset$). The simplest example of a Heegaard splitting is $M = S^3$ decomposed into two compression bodies $C_{1,0}^{(1)} = ST^2$, $C_{1,0}^{(2)} = ST^2$ (solid tori) which are glued along the boundary tori T^2 twisted by the modular S-transformation in $\text{MCG}(T^2) \cong SL(2,\mathbb{Z})$, although the partition function of S^3 is not computable in VTQFT as mentioned above.

The VTQFT path-integral produces a state $\left|Z_{\text{Vir}}\big(C_{g,n}(g_1, n_1; \cdots; g_m, n_m)\big)\right\rangle$ for the compression body, inserting a complete set of states $\left|\mathcal{F}_{g_i,n_i}^{\mathcal{C}_i}(\boldsymbol{p}_i)\right\rangle$ on each inner boundary component and a certain state $\left|\Phi_{g,n}^{\mathcal{C}}(\boldsymbol{p}_1, \cdots, \boldsymbol{p}_m; \boldsymbol{q})\right\rangle$ on the outer boundary

$$\left|Z_{\text{Vir}}\big(C_{g,n}(g_1, n_1; \cdots; g_m, n_m)\big)\right\rangle \tag{2.28}$$
$$:= \int \prod_{i=1}^m \left(d^{3g_i-3+n_i}\boldsymbol{p}_i \; \rho_{g_i,n_i}^{\mathcal{C}_i}(\boldsymbol{p}_i)\right) \left|\mathcal{F}_{g_1,n_1}^{\mathcal{C}_1}(\boldsymbol{p}_1)\right\rangle \otimes \cdots \otimes \left|\mathcal{F}_{g_m,n_m}^{\mathcal{C}_m}(\boldsymbol{p}_m)\right\rangle \otimes \left|\Phi_{g,n}^{\mathcal{C}}(\boldsymbol{p}_1, \cdots, \boldsymbol{p}_m : \boldsymbol{q})\right\rangle.$$

Technically, $\left|\Phi_{g,n}^{\mathcal{C}}(\boldsymbol{p}_1, \cdots, \boldsymbol{p}_m; \boldsymbol{q})\right\rangle$ is constructed by placing the network of Wilson lines $\boldsymbol{p}_i$ on the sub-channel $\mathcal{C}_i$ of $\mathcal{C}$ corresponding to the inner boundary block $\left|\mathcal{F}_{g_i,n_i}^{\mathcal{C}_i}(\boldsymbol{p}_i)\right\rangle$, and it may or may not contain additional network of Wilson lines $\boldsymbol{q}$ (see Figure 7 in Ref. [12]). The following example illustrates the process carried out here in more detail. The path-integral
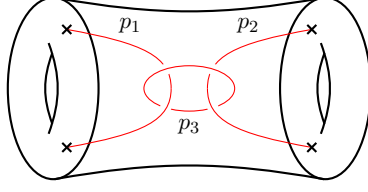
Figure 1. $\Sigma_{1,2} \times [0,1]$ wormhole with three Wilson lines tangling in the bulk

on the wormhole (2.27) serves as an example of this compression body path-integral with $m = 1$, $g_1 = g$, $n_1 = n$ and no additional Wilson lines $\boldsymbol{q}$. The two compression bodies are then glued together along their outer boundary $\Sigma_{g,n}$ twisted by γ. We evaluate the matrix element $\langle \Phi^{\mathcal{C}}_{g,n}(\boldsymbol{p}_1, \cdots, \boldsymbol{p}_{m_1}; \boldsymbol{q}_1) | U_{g,n}(\gamma) | \Phi^{\mathcal{D}}_{g,n}(\boldsymbol{q}_1, \cdots, \boldsymbol{q}_{m_2}; \boldsymbol{q}_2) \rangle$ and obtain

$$
\begin{aligned}
|Z_{\mathrm{Vir}}(M)\rangle &= \big\langle Z_{\mathrm{Vir}}\big(C^{(1)}_{g,n}(g_1, n_1; \cdots; g_{m_1}, n_{m_1})\big) \big| U(\gamma) \big| Z_{\mathrm{Vir}}\big(C^{(2)}_{g,n}(h_1, k_1; \cdots; h_{m_2}, k_{m_2})\big) \big\rangle \\
&:= \int \prod_{i=1}^{m_1} \big(d^{3g_i - 3 + n_i} \boldsymbol{p}_i \; \rho^{\mathcal{C}_i}_{g_i, n_i}(\boldsymbol{p}_i)\big) \int \prod_{j=1}^{m_2} \big(d^{3h_j - 3 + k_j} \boldsymbol{q}_j \; \rho^{\mathcal{D}_j}_{h_j, k_j}(\boldsymbol{q}_j)\big) \\
&\quad \times \big\langle \Phi^{\mathcal{C}}_{g,n}(\boldsymbol{p}_1, \cdots, \boldsymbol{p}_{m_1}; \boldsymbol{q}_1) \big| U_{g,n}(\gamma) \big| \Phi^{\mathcal{D}}_{g,n}(\boldsymbol{q}_1, \cdots, \boldsymbol{q}_{m_2}; \boldsymbol{q}_2) \big\rangle \\
&\quad \times \big| \mathcal{F}^{\mathcal{C}_1}_{g_1, n_1}(\boldsymbol{p}_1) \big\rangle \otimes \cdots \otimes \big| \mathcal{F}^{\mathcal{C}_{m_1}}_{g_{m_1}, n_{m_1}}(\boldsymbol{p}_{m_1}) \big\rangle \otimes \big| \mathcal{F}^{\mathcal{D}_1}_{h_1, k_1}(\boldsymbol{q}_1) \big\rangle \otimes \cdots \otimes \big| \mathcal{F}^{\mathcal{D}_{m_2}}_{h_{m_2}, k_{m_2}}(\boldsymbol{q}_{m_2}) \big\rangle.
\end{aligned}
\tag{2.29}
$$

In most cases, we only take into account the trivial gluing $U_{g,n}(\gamma) = \mathrm{id}_{\mathcal{H}_{g,n}}$.

Example: $\Sigma_{1,2} \times [0,1]$ wormhole with non-trivial bulk linking

To provide clarity, let us do an exercise in computing the VTQFT partition function for a particular geometry that has not yet appeared in the literature, namely $\Sigma_{1,2} \times [0,1]$ wormhole geometry with Wilson lines non-trivially linking in the bulk as seen in Figure 1. From this point onward, we will adopt the following shorthand notation to avoid unnecessary complications,

$$
C_{ijk} := C_0(p_i, p_j, p_k).
\tag{2.30}
$$

Let us first untangle the link by fusion kernal transformation and braiding

$$
\begin{aligned}
\left| \left(\vcenter{\hbox{}} \right) \right\rangle &= \int_0^\infty dp\, dp' \, F_{\mathbb{1}p} \begin{bmatrix} p_3 & p_1 \\ p_3 & p_1 \end{bmatrix} F_{\mathbb{1}p'} \begin{bmatrix} p_2 & p_3 \\ p_2 & p_3 \end{bmatrix} \left| \left(\vcenter{\hbox{}} \right) \right\rangle \\
&= \int_0^\infty dp\, dp' \, F_{\mathbb{1}p} \begin{bmatrix} p_3 & p_1 \\ p_3 & p_1 \end{bmatrix} F_{\mathbb{1}p'} \begin{bmatrix} p_2 & p_3 \\ p_2 & p_3 \end{bmatrix} e^{2\pi i (h_p - h_{p'} - h_1 + h_2)} \left| \left(\vcenter{\hbox{}} \right) \right\rangle
\end{aligned}
\tag{2.31}
$$

We denote as M the 3-manifold with two 2-punctured torus boundaries in the last line. Although M itself is a compression body, we would better Heegaard-split it along the dashed line into two compression bodies M_1 and M_2 shown in Figure 2. To implement the

Figure 2. Two compression bodies that constitute the boundary of the wormhole

VTQFT path-integral on them, one needs to apply the general path-integral rule (2.28)

$$|M_1\rangle = \int_0^\infty dp_a dp_b \, \rho_0(p_a)\rho_0(p_b)C_{ab3}^2 \left| \begin{matrix} p_a \\ p_3 \quad p_b \quad p_3 \end{matrix} \right\rangle \otimes \left| \begin{matrix} p_3\,p_1 \quad p_a \quad p_1\,p_3 \\ p_b \\ p \end{matrix} \right\rangle,$$

$$|M_2\rangle = \int_0^\infty dp_c dp_d \, \rho_0(p_c)\rho_0(p_d)C_{cd3}^2 \left| \begin{matrix} p_c \\ p_3 \quad p_d \quad p_3 \end{matrix} \right\rangle \otimes \left| \begin{matrix} p_3\,p_2 \quad p_c \quad p_2\,p_3 \\ p_d \\ p' \end{matrix} \right\rangle. \tag{2.32}$$

Both $|M_1\rangle$ and $|M_2\rangle$ are states in $\mathcal{H}_{1,2} \otimes \mathcal{H}_{1,2}$ and the blue lines p, p' correspond to the additional lines $\boldsymbol{q}$ in eq. (2.28). The outer boundary (colored in olive) has seemingly complicated network of Wilson lines because of p, p', but it can easily resolved by fusion transformation and the Wilson trianlge identity (2.23)

$$\left| \begin{matrix} p_a \\ p_3\,p_1 \quad p_b \quad p_1\,p_3 \\ p \end{matrix} \right\rangle = \int_0^\infty dp_e \, F_{pp_e}\begin{bmatrix} p_1 & p_1 \\ p_3 & p_3 \end{bmatrix} \left| \begin{matrix} p_a \\ p_b \\ p_3 \quad p_1 \quad p_1 \quad p_3 \\ p_e \end{matrix} \right\rangle$$

$$= \int_0^\infty dp_e \, F_{pp_e}\begin{bmatrix} p_1 & p_1 \\ p_3 & p_3 \end{bmatrix} \frac{1}{\rho_0(p_e)C_{11e}} F_{p_b p_e}\begin{bmatrix} p_a & p_a \\ p_1 & p_1 \end{bmatrix} \left| \begin{matrix} p_a \\ p_3 \quad p_e \quad p_3 \end{matrix} \right\rangle. \tag{2.33}$$

We thus take an inner product between outer boundaries of M_1 and M_2 to glue them together into M with $U_{g,n}(\gamma) = \mathrm{id}_{\mathcal{H}_{g,n}}$

$$|M\rangle = \int_0^\infty dp_a dp_b dp_c dp_d \, \rho_0(p_a)\rho_0(p_b)\rho_0(p_c)\rho_0(p_d)C_{ab3}^2 C_{cd3}^2$$

$$\times \left\langle \begin{matrix} p_a & p_c \\ p_3\,p_1 \quad p_b \quad p_1\,p_3 \quad p_3\,p_2 \quad p_d \quad p_2\,p_3 \\ p & p' \end{matrix} \right| \left| \begin{matrix} p_a \\ p_3 \quad p_b \quad p_3 \end{matrix} \right\rangle \otimes \left| \begin{matrix} p_c \\ p_3 \quad p_d \quad p_3 \end{matrix} \right\rangle$$

$$= \int_0^\infty dp_a dp_b dp_d dp_e \, \frac{\rho_0(p_a)\rho_0(p_b)\rho_0(p_d)C_{ab3}^2 C_{ad3}^2}{\rho_0(p_e)^3 C_{11e}C_{22e}C_{33e}C_{aae}} F_{pp_e}\begin{bmatrix} p_1 & p_1 \\ p_3 & p_3 \end{bmatrix} F_{p_b p_e}\begin{bmatrix} p_a & p_a \\ p_1 & p_1 \end{bmatrix}$$

$$\times F_{p'p_e}\begin{bmatrix} p_2 & p_2 \\ p_3 & p_3 \end{bmatrix} F_{p_d p_e}\begin{bmatrix} p_a & p_a \\ p_2 & p_2 \end{bmatrix} \left| \begin{matrix} p_a \\ p_3 \quad p_b \quad p_3 \end{matrix} \right\rangle \otimes \left| \begin{matrix} p_a \\ p_3 \quad p_d \quad p_3 \end{matrix} \right\rangle. \tag{2.34}$$

where eq. (2.13) is used from the first to the second line. Substituting this into (2.31) and applying the formula (A.20) followed by its complex conjugated version yield

$$
\left| \left\langle \text{} \right\rangle \right| = \frac{1}{\rho_0(p_3)^2} \int_0^\infty dp_a dp_b dp_d dp_e \, \frac{\rho_0(p_a)\rho_0(p_b)\rho_0(p_d)C_{ab3}^2 C_{ad3}^2}{\rho_0(p_e)C_{33e}C_{aae}} \quad (2.35)
$$

$$
\times S_{p_1 p_3}[p_e] S_{p_2 p_3}^*[p_e] F_{p_b p_e}\begin{bmatrix} p_a & p_a \\ p_1 & p_1 \end{bmatrix} F_{p_d p_e}\begin{bmatrix} p_a & p_a \\ p_2 & p_2 \end{bmatrix} \left| \text{} \right\rangle \otimes \left| \text{} \right\rangle .
$$

2.3   Consistency check: solid torus geometry

With the necessary tools available, we now go on to verify the effectiveness of VTQFT in the case of a simple geometry. Matching the VTQFT path-integral of wormhole geometries to ensemble CFT data has been explored extensively in the literature [13, 18, 39], so we focus on evaluating the solid torus case here. Solid torus is the most elementary yet momentous topology in 3d geometry as it encompasses both the thermal AdS$_3$ and the Euclidean BTZ blackhole [40]. Let us first review how to determine the torus moduli parameter τ for the thermal AdS$_3$ and the BTZ blackhole, which allows us to compute the VTQFT partition function $Z_{\text{Vir}}(ST^2; \tau) = \langle \tau | Z_{\text{Vir}}(ST^2) \rangle$ in the subsequent calculations.

The metric for the Euclidean AdS$_3$ with temperature T_H and Euclidean BTZ blackhole are given by

$$
g_{\text{AdS}_3} = \left(1 + \frac{r^2}{l^2} \right) dt_E^2 + \frac{1}{1 + \frac{r^2}{l^2}} dr^2 + r^2 d\theta, \quad (2.36)
$$

$$
g_{\text{BTZ}} = f(r)^2 dt_E^2 + \frac{1}{f(r)^2} dr^2 + r^2 \left(-\frac{J_E}{2r^2} dt_E + d\theta \right)^2, \quad (2.37)
$$

where $f(r) := \sqrt{-M + \frac{r^2}{l^2} - \frac{J_E^2}{4r^2}}$, $J_E := -iJ$ and $\theta \in [0, 2\pi)$. Note that AdS$_3$ is the special case $M = -1$ and $J_E = 0$ in the family of BTZ blackholes parametrized by M, J_E. The BTZ blackhole has two horizons corresponding to the solution of $f(r) = 0$, namely

$$
r_\pm := \sqrt{\frac{Ml^2 \pm l\sqrt{M^2 l^2 + J_E^2}}{2}} = \frac{1}{2}\left(\sqrt{l(Ml + J)} \pm \sqrt{l(Ml - J)} \right). \quad (2.38)
$$

Located at the outer radius r_+ is the event horizon whose surface area A is computed by a volume integral in terms of the induced metric $\widetilde{g}_{\text{event horizon}} := g_{\text{BTZ}}\big|_{r=r_+, \, t_E=const.} = r_+^2 d\theta^2$

$$
A = \int_0^{2\pi} d\theta \, \sqrt{\widetilde{g}_{\text{event horizon}}(\partial_\theta, \partial_\theta)} = 2\pi r_+. \quad (2.39)
$$

Viewed as a function of mass M and angular momentum J the exterior derivative dA is a linear combination of dM and dJ, and we can arrange it to

$$
dM = \frac{1}{lr_+}\left(\frac{2}{\pi l}(r_+^2 - r_-^2)dA + r_- dJ \right). \quad (2.40)
$$

This is nothing other than the first law of blackhole thermodynamics and we can read off the Hawking temperature

$$
T_H := \frac{1}{\beta_H} := \frac{r_+^2 - r_-^2}{2\pi l^2 r_+} = \frac{\sqrt{M^2 l^2 - J^2}}{\pi l(\sqrt{l(Ml + J)} + \sqrt{l(Ml - J)})}. \quad (2.41)
$$

Alternatively, this result can be inferred by analyzing the near-horizon geometry and identifying the periodicity of the Euclidean time required to eliminate the conical singularities at the event horizon.[5]

After the coordinate transfomations [41]

$$y_A := \sqrt{\frac{l^2}{r^2 + l^2}}\, e^{\frac{t_E}{l}}, \quad z_A := \sqrt{\frac{r^2}{r^2 + l^2}}\, e^{\frac{t_E}{l} - i\theta}, \quad \overline{z}_A := \sqrt{\frac{r^2}{r^2 + l^2}}\, e^{\frac{t_E}{l} + i\theta}, \qquad (2.43)$$

$$y_B := \sqrt{\frac{r_+^2 - r_-^2}{r^2 - r_-^2}}\, e^{\frac{r_+}{l}\theta - \frac{ir_-}{l^2} t_E}, \quad z_B := \sqrt{\frac{r^2 - r_+^2}{r^2 - r_-^2}}\, e^{\frac{2\pi r_+}{r_+ + r_-} T_H (l\theta + it_E)}, \quad \overline{z}_B := \sqrt{\frac{r^2 - r_+^2}{r^2 - r_-^2}}\, e^{\frac{2\pi r_+}{r_+ - r_-} T_H (l\theta - it_E)},$$

the metric of the theraml AdS_3 (2.36) and a Euclidean BTZ blackhole (2.37) read in Poincaré coordinates

$$g_{AdS_3} = \frac{l^2}{y_A^2}(dy_A^2 + dz_A d\overline{z}_A), \quad g_{BTZ} = \frac{l^2}{y_B^2}(dy_B^2 + dz_B d\overline{z}_B). \qquad (2.44)$$

We mainly consider the non-rotating BTZ blackhole ($J = 0$) in the subsequent discussion, where $r_- = 0$. For the spatial asymptotic regime $y_A \to 0$ and $y_B \to 0$ (or equivalently $r \to \infty$), their boundary coordinates z_A, z_B are

$$\lim_{r \to \infty} z_A = e^{\frac{t_E}{l} - i\theta}, \quad \lim_{r \to \infty} z_B = e^{2\pi T_H (l\theta + it_E)}, \qquad (2.45)$$

that have to be identified periodically as $z_A \sim e^{\frac{\beta_H}{l}} z_A$ and $z_B \sim e^{\frac{4\pi^2 l}{\beta_H}} z_B$ due to the periodicity $t_E \sim t_E + \beta_H$, $\theta \sim \theta + 2\pi$ of the original coordinates. If we introduce the new complex coordinates

$$w_A := \frac{i}{2\pi} \log \lim_{r \to \infty} z_A = \frac{\theta}{2\pi} + i\frac{t_E}{2\pi l}, \qquad (2.46)$$

$$w_B := \frac{i}{2\pi} \log \lim_{r \to \infty} z_B = -T_H t_E + il T_H \theta, \qquad (2.47)$$

they are the coordinates on tori as expected, with periodicity being $w_A \sim w_A + 1 \sim w_A + \tau_{AdS_3}$ and $w_B \sim w_B + 1 \sim w_B + \tau_{BTZ}$ where the moduli parameters are

$$\tau_{AdS_3} := \frac{\beta_H}{2\pi l} i, \quad \tau_{BTZ} := \frac{2\pi l}{\beta_H} i. \qquad (2.48)$$

They are related through modular S-transformation $\tau_{BTZ} = -\frac{1}{\tau_{AdS_3}}$.

Hawking-Page phase transition

As an initial demonstration of its validity, let us analyze how VTQFT replicates the 3d version of the Hawking-Page phase transition [42]. The derivation from the classical action is elegantly reviewed in [43].

---

[5]Use the coordinate $\rho^2 := r - r_+$ and approximate $f(r)$ to the second order in ρ. The metric (2.37) reads

$$g_{BTZ} = \Big(\frac{4r_+}{l^2} - \frac{2M}{r_+} + \mathcal{O}(\rho^2)\Big)\rho^2 dt_E^2 + \frac{4}{\frac{4r_+}{l^2} - \frac{2M}{r_+} + \mathcal{O}(\rho^2)} d\rho^2 + \cdots. \qquad (2.42)$$

Remove the conical singularities at $\rho = 0$ just as to eliminate the one at the origin of polar coordinates.

From eq. (2.2), the torus Virasoro character is the overlap between the moduli parameter basis $|\tau\rangle$ and the torus conformal block $|\chi_p\rangle = |\mathcal{F}_{1,0}(p)\rangle$

$$\chi_p(\tau) = \langle\tau|\chi_p\rangle. \tag{2.49}$$

The Virasoro character for vacuum and for the momentum above threshold $\frac{c-1}{24}$ are

$$\chi_0(\tau) = \frac{q^{-\frac{c-1}{24}}(1-q)}{\eta(\tau)}, \qquad \chi_p(\tau) := \frac{q^{p^2}}{\eta(\tau)} \; (p \in \mathbb{R}_{\geq 0}), \tag{2.50}$$

where $q := e^{2\pi i \tau}$ and $\eta(\tau) := q^{\frac{1}{24}} \prod_{n=1}^{\infty}(1-q^n)$ is the Dedekind eta function. The vacuum character has the extra factor $(1-q)$ due to the existence of a null state in the first level of its highest weight representation. As we see in eq. (2.48), the boundary moduli for thermal AdS_3 and non-rotating BTZ blackhole are each given by $\tau_{\mathrm{AdS}_3} := \frac{\beta_H}{2\pi l}i$, $\tau_{\mathrm{BTZ}} := -\frac{1}{\tau_{\mathrm{AdS}_3}}$, and by the VTQFT path-integral rule on handlebodies (2.26), their VTQFT partition functions are expressed as

$$Z_{\mathrm{Vir}}(\text{thermal AdS}_3) := Z_{\mathrm{Vir}}\left(ST^2; \tau_{\mathrm{AdS}_3}\right) = \chi_0(\tau_{\mathrm{AdS}_3}), \tag{2.51}$$

$$Z_{\mathrm{Vir}}(\text{BTZ}) := Z_{\mathrm{Vir}}\left(ST^2; -\tfrac{1}{\tau_{\mathrm{AdS}_3}}\right) = \chi_0\left(-\tfrac{1}{\tau_{\mathrm{AdS}_3}}\right). \tag{2.52}$$

It is worth noting that the BTZ partition function (2.52) is the vacuum Virasoro character in the dual channel ($\tau' = -\frac{1}{\tau}$), in exact agreement with the main proposal in Subsection 2.3 of Ref. [44]. The thermodynamical free energy for each geometry is

$$F_{\text{thermal AdS}_3} := -\frac{1}{\beta_H}\log\left|Z_{\mathrm{Vir}}(\text{thermal AdS}_3)\right|^2 = -\frac{1}{\beta_H}\log\left|\chi_0(\tau_{\mathrm{AdS}_3})\right|^2, \tag{2.53}$$

$$F_{\mathrm{BTZ}} := -\frac{1}{\beta_H}\log\left|Z_{\mathrm{Vir}}(\mathrm{BTZ})\right|^2 = -\frac{1}{\beta_H}\log\left|\chi_0\left(-\tfrac{1}{\tau_{\mathrm{AdS}_3}}\right)\right|^2. \tag{2.54}$$

It is evident that they coincide at the self-dual point

$$\tau_{\mathrm{AdS}_3} = -\frac{1}{\tau_{\mathrm{AdS}_3}} \iff \beta_H = 2\pi l, \tag{2.55}$$

but indeed more is true. Consider the difference of the free energies (2.53) and (2.54)

$$\begin{aligned} f(\beta_H) &:= F_{\mathrm{BTZ}} - F_{\text{thermal AdS}_3} \\ &= \frac{2}{\beta_H}\log|1-\tilde{q}| + \frac{2}{\beta_H}\log|1-q| - \frac{\pi^2 l(c-1)}{3\beta_H^2} + \frac{c-1}{12l} \qquad (\tilde{q} := e^{-\frac{2\pi i}{\tau}}) \\ &= \frac{1}{\beta_H}\log\left(\frac{1-e^{-\frac{\beta_H}{l}}}{1-e^{-\frac{4\pi^2 l}{\beta_H}}}\right)^2 - \frac{\pi^2 l(c-1)}{3\beta_H^2} + \frac{c-1}{12l}. \end{aligned} \tag{2.56}$$

This function is inherently vanishing at the self-dual point (2.55). A natural question is whether there exists any other vanishing point, i.e. a phase transition point, and it turns out that the answer is negative. Indeed, the equation $f(\beta_H) = 0$ is equivalent to $g(x) = 0$ ($x := \frac{\beta_H}{l}$), where

$$g(x) := \frac{1-e^{-x}}{1-e^{-\frac{4\pi^2}{x}}} - e^{(c-1)\left(\frac{\pi^2}{6x} - \frac{x}{24}\right)}, \tag{2.57}$$

and $g(x)$ is monotonically increasing as

$$g'(x) = \frac{e^{-x}}{1 - e^{-\frac{4\pi^2}{x}}} + \frac{4\pi^2 e^{-\frac{4\pi^2}{x^2}}(1 - e^{-x})}{x^2\left(1 - e^{-\frac{4\pi^2}{x^2}}\right)^2} + (c-1)\left(\frac{\pi^2}{6x^2} + \frac{1}{24}\right)e^{(c-1)\left(\frac{\pi^2}{6x} - \frac{x}{24}\right)} > 0, \quad (2.58)$$

for any $x > 0$ provided $c > 1$. Note that $c \leq 1$ is impossible for real b (see eq. (2.4)). Thus, we show that within VTQFT formulation, the phase transition occurs precisely once not only in the semiclassical regime $c = \frac{3l}{2G} + \mathcal{O}(1)$ $(G \to 0)$, but also when the central charge c has an arbitrary *finite* value above 1.

Bekenstein-Hawking entropy

We next address the Bekenstein-Hawking entropy for BTZ black hole. This begins with expanding the VTQFT partition function of the BTZ blackhole (2.52) in terms of the S-dual AdS$_3$ partition functions (2.51) with a Wilson line insertion p using eqs. (A.25), (2.50)

$$|Z_{\text{Vir}}(\text{BTZ})|^2 = \int_0^\infty dp d\overline{p}\, S_{\mathbb{1}p}[\mathbb{1}]S_{\mathbb{1}\overline{p}}^*[\mathbb{1}]\chi_p(\tau_{\text{AdS}_3})\chi_{\overline{p}}(-\overline{\tau}_{\text{AdS}_3})$$

$$= 32\int_0^\infty dp d\overline{p}\, \sinh(2\pi bp)\sinh\left(2\pi\frac{p}{b}\right)\sinh(2\pi b\overline{p})\sinh\left(2\pi\frac{\overline{p}}{b}\right)\frac{e^{-\frac{\beta}{l}(p^2 + \overline{p}^2)}}{|\eta(\tau_{\text{AdS}})|^2}. \quad (2.59)$$

In computing the thermal entropy, the main concern at present is the semiclassical limit $b \to +0$ $(G \to +0)$, where $\sinh(2\pi bp) = 2\pi bp + \mathcal{O}(b^2)$, $\sinh\left(2\pi\frac{p}{b}\right) = \frac{1}{2}e^{\frac{2\pi p}{b}} + \mathcal{O}(1)$. Then the partition function reduces to leading order to

$$|Z_{\text{Vir}}(\text{BTZ})|^2 \approx \frac{32\pi^2 b^2}{|\eta(\tau_{\text{AdS}_3})|^2}e^{\frac{2\pi^2 l}{\beta b^2}}\int_0^\infty dp d\overline{p}\, p\overline{p}\, e^{-\frac{\beta}{l}(p - \frac{\pi l}{\beta b})^2 - \frac{\beta}{l}(\overline{p} - \frac{\pi l}{\beta b})^2}$$

$$= \frac{32\pi^2 b^2}{|\eta(\tau_{\text{AdS}_3})|^2}e^{\frac{2\pi^2 l}{\beta b^2}}\frac{l^2}{4\beta^2}\left(\sqrt{\frac{\beta}{l}}\pi \cdot \frac{\pi l}{\beta b} + \mathcal{O}(1)\right)^2. \quad (2.60)$$

From the first to the second line, we employ the integral formula

$$\int dx\, x e^{-a(x-b)^2} = -\frac{1}{2a}\left(e^{-a(x-b)^2} + \sqrt{a}\pi b\, \text{erf}\left(\sqrt{a}(b-x)\right)\right) \qquad (a, b > 0), \quad (2.61)$$

and the fact that $\text{erf}(x) = \mathcal{O}(1)$ $(x \to \infty)$, where $\text{erf}(x)$ is the error function $\text{erf}(x) := \frac{2}{\sqrt{\pi}}\int_0^x dt\, e^{-t^2}$. The thermal entropy is obtained as

$$S := \left(1 - \beta\frac{\partial}{\partial\beta}\right)\log|Z_{\text{Vir}}(\text{BTZ})|^2 = \frac{4\pi^2 l}{\beta b^2} + O(1). \quad (2.62)$$

Bearing in mind that $r_- = 0$ in non-rotating case, we show by eq. (2.41) that to leading order in $b \approx \sqrt{\frac{4G}{l}}$ (see eq. (2.3))

$$S \approx 4\pi^2 l \cdot \frac{r_+}{2\pi l^2} \cdot \frac{l}{4G} = \frac{2\pi r_+}{4G}. \quad (2.63)$$

Therefore, VTQFT certainly provides a correct semiclassical result.

3 Anyon condensation in modular tensor category

Anyon condensation [45] is a generalization of the gauging invertible symmetries to non-invertible cases. For invertible symmetries, suppose $G^{(p)}$ is a group representing p-form symmetry of a theory, a transformation acting on p-dimensional (possibly non-local) operators in the theory. The theory is gauged by selecting a subgroup of $G^{(p)}$ that does not carry a 't Hooft anomaly and promoting the background gauge field to a dynamical variable. More specifically, the process involves summing over inequivalent $(p+1)$-chains if $G^{(p)}$ is discrete, or performing a path-integral over a $(p + 1)$-form not connected by gauge transformations if $G^{(p)}$ is continuous. For general aspects of gauging invertible symmetries, see Section 3 and 4 in the excellent review [46]. In the non-invertible case, the fusion rule of codimension $(p + 1)$ operators acting as p-form symmetries becomes non-invertible, for which the symmetry is represented not by a group but more generally by a category. Hence, non-invertible symmetries are often referred to as categorical symmetries. Anyon condensation is therefore formulated as a generalization of gaugeing 1-form symmetry for non-invertible symmetries.

3.1 3d non-Abelian TQFT and Lagrangian algebra object

In this subsection, we summarize the detailed procedures of anyon condensation, which is also reviewed in Subsection 4.3 in Ref. [21] for 2d theories, and in Subsection 3.1 - 3.2 in Ref. [47], Subsection 4.1 in Ref. [23], Subsection 7.1 in Ref. [48] for 3d TQFT. Recent developments include, for example, Ref. [49, 50].

Let $\mathcal{C}$ be a modular tensor category associated with a 3d TQFT and $\mathcal{I}(\mathcal{C})$ is the label set of simple objects in $\mathcal{C}$. A modular tensor category $\mathcal{C}$ is a $\mathbb{C}$-*linear semisimple finite ribbon category*, where the simple objects in $\mathcal{C}$ are Wilson lines labeled by $\mathcal{I}(\mathcal{C})$ representing the fundamental excitations in 3d TQFT. Each condition defining a modular tensor category corresponds physically to the existence of a finite family of inequivalent Wilson lines $(L_i)_{i \in \mathcal{I}(\mathcal{C})}$, the well-defined concept of product (fusion) between them, and the braiding, the exchange of different particles. See Appendix B for mathematical foundations and the relation among various categorical notions.

In considering anyon condensation, let us first introduce a specific object named algebra object in $\mathcal{C}$, which is defined for braided tensor categories in general. An **algebra object** in $\mathcal{C}$ is a triplet $(\mathcal{A}, m, \eta)$ consisting of an object $\mathcal{A} = \bigoplus_{i \in \mathcal{I}(\mathcal{C})} Z_i^{\mathcal{A}} L_i \in \mathrm{Obj}\,\mathcal{C}$ ($Z_i^{\mathcal{A}} \in \mathbb{Z}_{\geq 0}$), the **product morphism** $m : \mathcal{A} \otimes \mathcal{A} \to \mathcal{A}$ and the **unit morphism** $\eta : \mathbb{1} \to \mathcal{A}$ satisfying the **associativity** and the **unit axiom**

$$m \circ (m \otimes \mathrm{id}_{\mathcal{A}}) \circ \alpha_{\mathcal{A}, \mathcal{A}, \mathcal{A}} = m \circ (\mathrm{id}_{\mathcal{A}} \otimes m), \tag{3.1}$$

$$m \circ (\eta \otimes \mathrm{id}_{\mathcal{A}}) = \mathrm{id}_{\mathcal{A}} = m \circ (\mathrm{id}_{\mathcal{A}} \otimes \eta). \tag{3.2}$$

They are described pictorially as

$$\tag{3.3}$$

In an analogous fashion, a **co-algebra object** in $\mathcal{C}$ is a triplet $(\mathcal{A}, \Delta, \iota)$ where $\mathcal{A} \in \mathrm{Obj}\,\mathcal{C}$ is an object, $\Delta : \mathcal{A} \to \mathcal{A} \otimes \mathcal{A}$ is the **co-product morphism** and $\iota : \mathcal{A} \to \mathbb{1}$ is the **co-unit**

morphism, complying the **co-accosiativity** and the **co-unit axiom**

$$\Delta \circ (\Delta \otimes \mathrm{id}_{\mathcal{A}}) = \alpha_{\mathcal{A},\mathcal{A},\mathcal{A}} \circ \Delta \circ (\mathrm{id}_{\mathcal{A}} \otimes \Delta), \tag{3.4}$$

$$(\mathrm{id}_{\mathcal{A}} \otimes \iota) \circ \Delta = \mathrm{id}_{\mathcal{A}} = (\iota \otimes \mathrm{id}_{\mathcal{A}}) \circ \Delta, \tag{3.5}$$

expressed as the same diagram as eq. (3.3) but with their orientation reversed vertically

$$\tag{3.6}$$

If $\mathcal{A}$ is both an algebra object and a co-algebra object in $\mathcal{C}$, it must fulfill further conditions to be condensable. The first one is the **separability**

$$m \circ \Delta = c \cdot \mathrm{id}_{\mathcal{A}} \ (\exists c \in \mathbb{Z}_{\geq 0}), \tag{3.7}$$

which states that fusing after branching is equivalent to doing nothing up to a constant factor:

$$\tag{3.8}$$

A separable algebra object is **connected** (or **haploid**) if

$$\dim \mathrm{Hom}_{\mathcal{C}}(\mathbb{1}, \mathcal{A}) = 1, \tag{3.9}$$

that is, $\mathcal{A}$ has only single identity object $\mathbb{1}$ in it. More complex is the **Frobenius condition**

$$(m \otimes \mathrm{id}_{\mathcal{A}}) \circ (\mathrm{id}_{\mathcal{A}} \otimes \Delta) = \Delta \circ m = (\mathrm{id}_{\mathcal{A}} \otimes m) \circ (\Delta \otimes \mathrm{id}_{\mathcal{A}}), \tag{3.10}$$

requiring the consistency under crossing:

$$\tag{3.11}$$

An algebra object $\mathcal{A}$ is **commutative** if

$$m = m \circ \theta_{\mathcal{A},\mathcal{A}}. \tag{3.12}$$

Graphically, it guarantees that $\mathcal{A}$ acquires no non-trivial phase after braiding

$$\tag{3.13}$$

Combining the above conditions, a ***condensable anyon*** in 3d TQFT is *a connected commutative separable Frobenius algebra object* $\mathcal{A} = \bigoplus_{i \in \mathcal{I}(\mathcal{C})} Z_i^{\mathcal{A}} L_i \in \mathrm{Obj}\,\mathcal{C}.$[6] A condensable anyon is ***Lagrangian*** if its quantum dimension (Frobenius-Perron dimension) $\dim \mathcal{A}$ equals to the total qunatum dimension $\mathcal{D} := \sqrt{\sum_{i \in \mathcal{I}(\mathcal{C})} \dim L_i}$ of the MTC $\mathcal{C}$. This is equivalent to asserting that $\mathcal{A}$ is the "maximal" object that can be condensed in the symmetry category, such that adding any other object in $\mathcal{C}$ to $\mathcal{A}$ breaks at least one of its defining properties (typically by inducing a non-trivial braiding phase). Just as gauging a Lagrangian subgroup of invertible symmetries generates a theory with a trivial bulk, condensing a Lagrangian condensable anyon produces a theory where the bulk is trivial.

The anyon condensation in question is achieved by placing the condensable anyons on a fine mesh over the spacetime manifold. For a general d-manifold $(d > 2)$ M, a ***fine mesh*** refers to the graph that is dual to the 1-skeleton formed by the vertices and edges of the d-simplices obtained from triangulating M. Specific examples, such as the case of handlebodies, are discussed in Subsection 3.2 of Ref. [23], and our main focus—the factorization—is demonstrated based on that within the context of Chern-Simons theory.

3.2 Diagonal Lagrangian condensable anyon

Consider the theory $\mathcal{C} \boxtimes \overline{\mathcal{C}}$, where $\overline{\mathcal{C}}$ corresponds to the orientation-reversal of the original 3d TQFT. In simple terms, all the crossing operations of $\overline{\mathcal{C}}$ are given by the complex conjugates of those of $\mathcal{C}$. In this subsection, we introduce the canonical condensable anyon associated with $\mathcal{C} \boxtimes \overline{\mathcal{C}}$, referred to as the diagonal Lagrangian condensable anyon. The symbol $\boxtimes$ here denotes the tensor product of multiple categories, known as ***Deligne's tensor product*** (see Section 1.11 in Ref. [51]), and is distinct from the symbol $\otimes$ used to fuse objects within a single category $\mathcal{C}$.

The ***diagonal Lagrangian condensable anyon*** is

$$\mathcal{A} := \bigoplus_{i \in \mathcal{I}(\mathcal{C})} L_i \boxtimes \overline{L}_i. \tag{3.14}$$

The algebra object $\mathcal{A}$ is manifestly commutative as the braiding phases originating from the chiral part and the anti-chiral part cancel out. Given the fusion rules among Wilson lines

$$L_i \otimes L_j = \bigoplus_k N_{ij}^k L_k \qquad (N_{ij}^k \in \mathbb{Z}_{\geq 0}), \tag{3.15}$$

the product morphism $m : \mathcal{A} \otimes \mathcal{A} \to \mathcal{A}$ is defined by

$$m := \bigoplus_{i,j,k,\alpha} m_{ij,\alpha}^k \boxtimes \overline{m}_{ij,\alpha}^k, \tag{3.16}$$

where $m_{ij,\alpha}^k \in \mathrm{Hom}_{\mathcal{C}}\left(L_i \otimes L_j, L_k\right)$, $\overline{m}_{ij,\alpha}^k \in \mathrm{Hom}_{\overline{\mathcal{C}}}\left(\overline{L}_i \otimes \overline{L}_j, \overline{L}_k\right)$ $(\alpha = 1, \cdots, N_{ij}^k)$ is the basis. The co-product morphism $\Delta : \mathcal{A} \to \mathcal{A} \otimes \mathcal{A}$ is given by

$$\Delta\left(\bigoplus_{i \in \mathcal{I}(\mathcal{C})} L_i \boxtimes \overline{L}_i\right) := \bigoplus_{i,j,k} N_{jk}^i \overline{N}_{jk}^i \left(L_j \boxtimes \overline{L}_j\right) \otimes \left(L_k \boxtimes \overline{L}_k\right). \tag{3.17}$$

---

[6]A condensable anyon in 2d, on the other hand, is a connected *symmetric* separable Frobenius algebra object [21].

The fact that the algebra object $(\mathcal{A}, m, \eta, \Delta, \iota)$ defined by eqs. (3.16), (3.17) is indeed condensable (technically a Frobenius algebra object) is guaranteed by Proposition 7.20.1 in Ref. [51].[7] The co-associativity and the co-unit axiom follow automatically once the Frobenius condition is satisfied.[8]

Example: $SU(2)_2$ Chern-Simons theory

Let us confirm that separability holds in the simplest non-Abelian case $SU(2)_2$. The Wilson lines in $SU(2)_k$ Chern-Simons theory are labeled by spin variables $j = 0, \frac{1}{2}, 1, \cdots, \frac{k}{2}$ of integrable representations, obeying the fusion rule

$$L_i \otimes L_j = \bigoplus_{k=|i-j|}^{\min\{i+j,\, k-(i+j)\}} L_k. \tag{3.18}$$

where j has an increment of 1 in the sum. In $k = 2$ case, it is explicitly written down as

$$L_0 \otimes L_0 = L_0, \;\; L_0 \otimes L_{\frac{1}{2}} = L_{\frac{1}{2}}, \;\; L_0 \otimes L_1 = L_1, \tag{3.19}$$

$$L_{\frac{1}{2}} \otimes L_{\frac{1}{2}} = L_0 \oplus L_1, \;\; L_{\frac{1}{2}} \otimes L_1 = L_{\frac{1}{2}}, \;\; L_1 \otimes L_1 = L_0. \tag{3.20}$$

This TQFT shares the same fusion rule as the Ising TQFT if we identify $L_{\frac{1}{2}}$ and L_1 with the Ising anyon σ and ψ. The diagonal Lagrangian algebra is

$$\mathcal{A} = L_0 \boxtimes \overline{L}_0 \oplus L_{\frac{1}{2}} \boxtimes \overline{L}_{\frac{1}{2}} \oplus L_1 \boxtimes \overline{L}_1 \tag{3.21}$$

and the co-product (3.17) maps $\mathcal{A}$ to

$$\Delta(\mathcal{A}) = (L_0 \boxtimes \overline{L}_0) \otimes (L_0 \boxtimes \overline{L}_0) \oplus 2(L_0 \boxtimes \overline{L}_0) \otimes (L_{\frac{1}{2}} \boxtimes \overline{L}_{\frac{1}{2}}) \oplus 2(L_0 \boxtimes \overline{L}_0) \otimes (L_1 \boxtimes \overline{L}_1)$$

$$\oplus 2(L_{\frac{1}{2}} \boxtimes \overline{L}_{\frac{1}{2}}) \otimes (L_{\frac{1}{2}} \boxtimes \overline{L}_{\frac{1}{2}}) \oplus 2(L_{\frac{1}{2}} \boxtimes \overline{L}_{\frac{1}{2}}) \otimes (L_1 \boxtimes \overline{L}_1) \oplus (L_1 \boxtimes \overline{L}_1) \otimes (L_1 \boxtimes \overline{L}_1) \tag{3.22}$$

so we conclude that

$$m \circ \Delta(\mathcal{A}) = 4\mathcal{A} \tag{3.23}$$

4 Anyon condensation in Virasoro TQFT

We extend anyon condensation to VTQFT with assciated category denoted as $\mathcal{C}$. $\mathcal{C}$ is a ribbon category, that is $\mathbb{C}$-linear Abelian rigid braided monoidal category with a ribbon structure (twist). However, it is not semisimple nor locally finite due to the inifinite number of Wilson lines (simple objects). In this way $\mathcal{C}$ is a non-semisimple non-locally finite $\mathbb{C}$-linear Abelian ribbon category, whose relative position is indicated by the green area in Figure 6 in Appendix B. In spite of these problems, we will define

$$\mathcal{A} := \int_{\mathbb{R}_{\geq 0}}^{\oplus} dp \, L_p \boxtimes \overline{L}_p \tag{4.1}$$

---

[7]Readers may refer the definition of dual morphisms like m^* and e^* appearing in Proposition 7.20.1 to eq. (2.47) and (2.48) (p.41) in this reference.

[8]We thank K. Ohmori for telling us this point.

and still call it the **_diagonal condensable anyon_**. The modifier "Lagrangian" is being removed because $\mathcal{A}$ does not contain the identity line $\mathbb{1} \boxtimes \mathbb{1}$. Although the continuous direct sums is not guaranteed in a mathematically rigorous manner, we leave it for the discussion in Section 5 for now. As stated in the introduction, VTQFT as a gravitational theory suffers from the factorization puzzle, the non-factorization of the partition function for geometries with multiple boundaries. We solve the paradox by condensating the VTQFT diagonal condensable anyon (4.1) for two-boundary wormhole geometries in line with the method described in Ref. [23].

4.1   Projector

In this subsection, we introduce a special link of Wilson lines that frequently appears in the anyon condensation proccess when the diagonal condensable anyon is placed along a fine mesh of a manifold. The link drastically simplify the computation of VTQFT path-integral. A **_projector_** is an object indicated in the l. h. s. of

$$ \text{(4.2)} $$

In contrast to Section 2, we use a single link diagram or single ket $| \cdot \rangle$ to represent the tensor product of the chiral part and the anti-chiral part, which is why we use the notation $L_{p_x} \boxtimes \overline{L}_{\overline{p}_x}$ in the above equation. From this point forward, we will adhere to this rule. The condensable anyon $\mathcal{A}$ (the red line) shown in this figure represents a superposition of its component. The concept of projector is first appeared in eq. (5.34) of Ref. [52] in the context of modular tensor category. The central point to be confirmed is that the projector is propotional to the r. h. s. of eq. (4.2), as briefly explained in the last paragraph of Subsection 4.1 in Ref. [23] in the case of Chern-Simons theory. To begin with, let us clarify that in this paper inserting the diagonal condensable anyon (4.1) means a superposition of each component weighted by $\rho_0(p_i)$ for each internal line p_i and C_{ijk} for each trivalent junctions ${}_i \!\!\downarrow_k^j$. Under this rule, the projector is presented as

$$ \text{(4.3)} $$

In this diagram, p_x and $\overline{p}_x$ are a different variables so that $L_{p_x} \boxtimes \overline{L}_{\overline{p}_x}$ is a general Wilson line in $\mathcal{C} \boxtimes \overline{\mathcal{C}}$ while $L_{p_i} \boxtimes \overline{L}_{p_i}$ are restricted to diagonal lines contained in $\mathcal{A}$. We then implement

fusion transformation with $L_{p_3} \boxtimes \overline{L}_{p_3}$ as the internal line to create the Verlinde loop

$$
\begin{aligned}
& \int_0^\infty dp_b d\overline{p}_a \, F_{p_3 p_a} \begin{bmatrix} p_1 & p_2 \\ p_4 & p_4 \end{bmatrix} F_{p_3 \overline{p}_a} \begin{bmatrix} p_1 & p_2 \\ p_4 & p_4 \end{bmatrix}
\end{aligned}
\tag{4.4}
$$

Performing the integration w.r.t. p_3 in eq. (4.3), utilizing eq. (A.16), and resolving the Verlinde loop by eq. (2.24) yield

$$
= \int_0^\infty dp_1 dp_2 dp_a \, \rho_0(p_4)\rho_0(p_a) C_{44a} C_{12a}
$$

$$
= \int_0^\infty dp_1 dp_2 dp_4 dp_a \, \rho_0(p_4)\rho_0(p_a) C_{44a} C_{12a} \frac{S_{p_4 p_x}[p_a] S^*_{p_4 \overline{p}_x}[p_a]}{S_{\mathbb{1} p_x}[\mathbb{1}] S_{\mathbb{1} \overline{p}_x}[\mathbb{1}]}
$$

$$
\tag{4.5}
$$

The crucial point is that eq. (A.16) applies in this case because the first subscript and the four arguments of the two fusion kernels are identical. The chiral part Liouville momentum p and the anti-chiral part Liouville momentum $\overline{p}$ are different in general, but they coincide due to the diagonalty of the condensable anyon $\mathcal{A}$. We then employ eq. (A.24) to exchange the subscripts of $S_{p_4 p_x}$ and perform the integration w.r.t. p_4 by eq. (A.6)

$$
= \int_0^\infty dp_1 dp_2 dp_a \, \rho_0(p_a) C_{xxa} C_{12a} \frac{\delta(p_x - \overline{p}_x)}{S_{\mathbb{1} p_x}[\mathbb{1}]}
\tag{4.6}
$$

Figure 3. The torus wormhole with the Wilson line insertion connecting the two boundaries. The dashed lines are the inner boundary $\Sigma_{1,1}$.

The graph in the integrand is further modified by the fusion transformation as

$$
\begin{array}{c} L_{p_1}\boxtimes\overline{L}_{p_1}\, L_{p_x}\boxtimes\overline{L}_{p_x} \\ \\ \\ L_{p_a}\boxtimes\overline{L}_{p_a} \\ \\ L_{p_2}\boxtimes\overline{L}_{p_2}\, L_{p_x}\boxtimes\overline{L}_{p_x} \end{array}
= \int_0^\infty dp_b d\overline{p}_b F_{p_a p_b}\begin{bmatrix} p_1 & p_x \\ p_2 & p_x \end{bmatrix} F_{p_a \overline{p}_b}\begin{bmatrix} p_1 & p_x \\ p_2 & p_x \end{bmatrix}
\begin{array}{c} L_{p_1}\boxtimes\overline{L}_{p_1}\, L_{p_x}\boxtimes\overline{L}_{p_x} \\ \\ L_{p_b}\boxtimes\overline{L}_{\overline{p}_b} \\ \\ L_{p_2}\boxtimes\overline{L}_{p_2}\, L_{p_x}\boxtimes\overline{L}_{p_x} \end{array} .
\tag{4.7}
$$

We ultimately establish the relation (4.2) by performing the integration w. r. t. p_a with the assistance of eq. (A.16)

$$
\begin{array}{c} \mathcal{A} \quad L_{p_x}\boxtimes\overline{L}_{\overline{p}_x} \\ \\ \mathcal{A} \qquad \mathcal{A} \\ \\ \mathcal{A} \end{array}
= \int_0^\infty dp_1 dp_2 dp_b\,\rho_0(p_b) C_{1xb} C_{2xb}\frac{\delta(p_x - \overline{p}_x)}{\rho_0(p_x)}
\begin{array}{c} L_{p_1}\boxtimes\overline{L}_{p_1}\, L_{p_x}\boxtimes\overline{L}_{p_x} \\ \\ L_{p_b}\boxtimes\overline{L}_{p_b} \\ \\ L_{p_2}\boxtimes\overline{L}_{p_2}\, L_{p_x}\boxtimes\overline{L}_{p_x} \end{array}
$$

$$
= \frac{\delta(p_x - \overline{p}_x)}{\rho_0(p_x)}
\begin{array}{c} \mathcal{A} \quad L_{p_x}\boxtimes\overline{L}_{p_x} \\ \\ \mathcal{A} \\ \\ \mathcal{A} \quad L_{p_x}\boxtimes\overline{L}_{p_x} \end{array} .
\tag{4.8}
$$

4.2 Factorization

Now that everything is in place, we will exemplify the factorization of the partition function of a wormhole geometry for two simple cases, the torus wormhole $T^2 \times [0,1]$ and the genus two wormhole $\Sigma_{2,0} \times [0,1]$ coupled to matter fields.

4.2.1 Torus wormhole

We avoid the pure torus wormhole $T^2 \times [0,1]$ and instead add the Wilson line $L_p\boxtimes\overline{L}_{\overline{p}}$ that connect the two boundaries, because the wormhole geometry $\Sigma_{g,0} \times [0,1]$ in general is non-hyperbolic for which the VTQFT partition function is possibly ill-behaved. Indeed,

one will find that there appears multiple divergent constant when computing the anyon condensation in the same way as what is done in the followng for pure $T^2 \times [0,1]$. The geometry is depicted in Figure 3 where the red lines represents the diagonal condensable anyons $\mathcal{A}$ placed on the fine mesh. The VTQFT path-integral (2.28) assigns it to a state

$$
\left| \vcenter{\hbox{}} \right\rangle = \int_0^\infty dp_x d\overline{p}_x \, \rho_0(p_x)\rho_0(\overline{p}_x) C_{xxp} C_{\overline{xxp}}
$$

$$
\times \left| \vcenter{\hbox{}} \right\rangle \otimes \left| \vcenter{\hbox{}} \right\rangle . \tag{4.9}
$$

Recall that the ket $|\cdot\rangle$ actually represents the tensor product of the chiral and the anti-chiral state, which accounts for the presence of the multiple integral by p_x, $\overline{p}_x$. We have to simplify the outer boundary state that contain the complicated network of condensable anyons $\mathcal{A}$. As mentioned earlier, we interpret the insertion of condensable anyons $\mathcal{A}$ as a superposition of its simple components toghether with $\rho_0(p_i)$ and C_{ijk} attached to each internal momentum and trivalent junction

$$
\left| \vcenter{\hbox{}} \right\rangle = \prod_{i=1}^3 \left(\int_0^\infty dp_i \, \rho_0(p_i) \right) C_{123}^2 \left| \vcenter{\hbox{}} \right\rangle . \tag{4.10}
$$

The projector formula (4.8) enables us to resolve the link on the left side of the genus, altering p_i $(i = 2, 3)$ integrals to p_α integrals as

$$
\prod_{i\in\{2,3\}} \left(\int_0^\infty dp_i \, \rho_0(p_i) \right) C_{123}^2 \left| \vcenter{\hbox{}} \right\rangle
$$

$$
= \frac{\delta(p_x - \overline{p}_x)}{\rho_0(p_x)} \int_0^\infty dp_\alpha \, \rho_0(p_\alpha) C_{1x\alpha}^2 \left| \vcenter{\hbox{}} \right\rangle \tag{4.11}
$$

$$
= \frac{\delta(p_x - \overline{p}_x)}{\rho_0(p_x)} \int_0^\infty dp_\alpha \, \frac{\rho_0(p_\alpha) C_{1x\alpha}^2}{\rho_0(p) C_{pxx} \rho_0(\overline{p}) C_{\overline{p}xx}} F_{p_1 p} \begin{bmatrix} p_\alpha & p_\alpha \\ p_x & p_x \end{bmatrix} F_{p_1 \overline{p}} \begin{bmatrix} p_\alpha & p_\alpha \\ p_x & p_x \end{bmatrix} \left| \vcenter{\hbox{}} \right\rangle .
$$

The p_1 integrals remain unchanged under this operation. It should be noted that in the second line the Wilson line $L_{p_x} \boxtimes \overline{L}_{\overline{p}_x}$ is projected onto the component $L_{p_x} \boxtimes \overline{L}_{p_x}$ of the diagonal condensable anyon (4.1) by virtue of the projectors. From the second to the third line, we apply the Wilson triangle identity (2.23). Using the forumula (A.16) to the dp_1 integral, the outer boundary state (4.10) reads

$$
\left| \vcenter{\hbox{}} \right\rangle = \frac{\delta(p_x - \overline{p}_x)}{\rho_0(p_x)} \int_0^\infty dp_\alpha \, \frac{C_{\alpha\alpha p} \delta(p - \overline{p})}{\rho_0(p) C_{pxx}} \left| \vcenter{\hbox{}} \right\rangle . \tag{4.12}
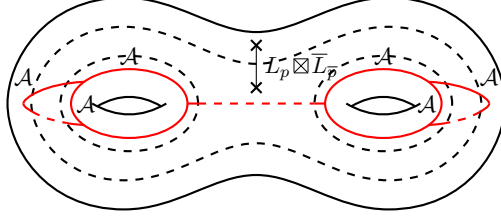$$

Figure 4. $\Sigma_{2,0} \times [0,1]$ wormhole with $\mathcal{A}$ inserted along its fine mesh. The dashed lines are the inner boundary $\Sigma_{2,0}$.

By substituting this result to eq. (4.9), we finally conclude that the partition function actually factorizes

$$
\left| \vcenter{\hbox{}} \right\rangle = \frac{\delta(p - \bar{p})}{\rho_0(p)} \int_0^\infty dp_x dp_\alpha \, \rho_0(p_x) \rho_0(p_\alpha) C_{xxp} C_{\alpha\alpha p}
$$

$$
\times \left| \vcenter{\hbox{}} \right\rangle \otimes \left| \vcenter{\hbox{}} \right\rangle
$$

$$
= \frac{\delta(p - \bar{p})}{\rho_0(p)} \left| \vcenter{\hbox{}} \right\rangle \otimes \left| \vcenter{\hbox{}} \right\rangle. \tag{4.13}
$$

As a repeated reminder, the insertion of condensable anyons is a superposition of the simple components with $\rho_0(p_i)$ and C_{ijk} assigned to each internal momentum and trivalent junction.

4.2.2 Genus two wormhole

The wormhole geometry $\Sigma_{2,0} \times [0,1]$ can be represented as a handlebody $S\Sigma_{2,0}$ with a smaller handlebody $S\Sigma'_{2,0}$ curved out from its interior. Just as the torus wormhole case, we consider $\Sigma_{2,0} \times [0,1]$ with a Wilson line (matter field) insertion as a probe instead of the pure $\Sigma_{2,0} \times [0,1]$ since $\Sigma_{2,0} \times [0,1]$ is non-hyperbolic, i.e. off shell. The Wilson line insertion and the fine mesh of $\Sigma_{2,0} \times [0,1]$ are illustrated in Figure 4. The path-integral rule on a compression body (2.28) prepares a state

$$
\left| \vcenter{\hbox{}} \right\rangle = \int_0^\infty dp_x d\bar{p}_x dp_y d\bar{p}_y dp_z d\bar{p}_z dp_w d\bar{p}_w \, \rho_0(p_x) \rho_0(\bar{p}_x) \rho_0(p_y) \rho_0(\bar{p}_y)
$$

$$
\times \rho_0(p_z) \rho_0(\bar{p}_z) \rho_0(p_w) \rho_0(\bar{p}_w) C_{xxz} C_{\overline{xxz}} C_{yyz} C_{\overline{yyz}} C_{pzw} C_{\overline{pzw}}
$$

$$
\times \left| \vcenter{\hbox{}} \right\rangle \otimes \left| \vcenter{\hbox{}} \right\rangle. \tag{4.14}
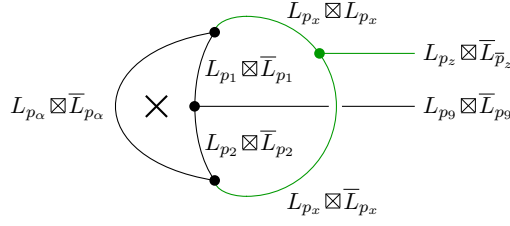$$

– 24 –

Figure 5. The left half of the link in eq. (4.16). The container manifold $\Sigma_{2,0}$ is ommited for simplicity and the X mark represents the location of the left genus.

The six-fold integral by $p_x, \overline{p}_x, \cdots, p_z, \overline{p}_z$ is due to the presence of both the chiral and the anti-chiral part. The subtlties arise from the outer boundary state with the network of condensable anyons $\mathcal{A}$ linking with the complete set of basis (the geen lines) in nontrivial ways. The superposition rule decompose the outer boundary state into the nine-fold integral over each simple component of the diagonal condensable anyon

$$\prod_{i=1}^{9}\left(\int_0^\infty dp_i\,\rho_0(p_i)\right)C_{134}C_{234}C_{129}C_{569}C_{578}C_{678}\left|\left(\begin{array}{c}\end{array}\right.\right. \tag{4.15}$$

Here we write (i,i) instead of $L_{p_i}\boxtimes\overline{L}_{p_i}$ for visibility. In order to reduce it to a more handleable form, we apply the projector formula (4.8) to both links near the two genera, altering p_i $(i=3,4,7,8)$ integrals to p, p' integrals as

$$\prod_{i\in\{3,4,7,8\}}\left(\int_0^\infty dp_i\,\rho_0(p_i)\right)C_{134}C_{234}C_{578}C_{678}\left|\left(\begin{array}{c}\end{array}\right.\right\rangle \tag{4.16}$$

$$=\int_0^\infty dp_\alpha dp_\beta\,\rho_0(p_\alpha)\rho_0(p_\beta)C_{1x\alpha}C_{2x\alpha}C_{5y\beta}C_{6y\beta}\frac{\delta(p_x-\overline{p}_x)\delta(p_y-\overline{p}_y)}{\rho_0(p_x)\rho_0(p_y)}\left|\left(\begin{array}{c}\end{array}\right.\right\rangle.$$

The p_i $(i=1,2,5,6,9)$ integrals remain unchanged under this operation. $(z,\overline{z})$ in the graph is a shorthand for $L_{p_z}\boxtimes\overline{L}_{\overline{p}_z}$. The line $L_{p_x}\boxtimes\overline{L}_{\overline{p}_x}$ (resp. $L_{p_y}\boxtimes\overline{L}_{\overline{p}_y}$) is restricted to the component $L_{p_x}\boxtimes\overline{L}_{p_x}$ (resp. $L_{p_y}\boxtimes\overline{L}_{p_y}$) of the diagonal condensable anyon (4.1) by virtue of the projectors while $L_{p_z}\boxtimes\overline{L}_{\overline{p}_z}$ is not. The result is still far from being refined, so let us further delve into a smaller part of the link as shown in Figure 5. There, we bisect the link in eq. (4.16) in the middle of the picture and only pick the left half. The objective is to attempt by some means to create the Wilson bubble to apply the formula (2.22). The procedure breaks down into the following three steps

$$
\times \int_0^\infty dp_a d\overline{p}_a \, F_{p_1 p_a} \begin{bmatrix} p_\alpha & p_2 \\ p_x & p_9 \end{bmatrix} F_{p_1 \overline{p}_a} \begin{bmatrix} p_\alpha & p_2 \\ p_x & p_9 \end{bmatrix} ,
$$

$$
\times \int_0^\infty dp_b d\overline{p}_b \, F_{p_2 p_b} \begin{bmatrix} p_\alpha & p_\alpha \\ p_a & p_x \end{bmatrix} F_{p_2 \overline{p}_b} \begin{bmatrix} p_\alpha & p_\alpha \\ \overline{p}_a & p_x \end{bmatrix} ,
$$

$$
\times \int_0^\infty dp_c d\overline{p}_c \, F_{p_a p_c} \begin{bmatrix} p_b & p_9 \\ p_x & p_x \end{bmatrix} F_{\overline{p}_a \overline{p}_c} \begin{bmatrix} \overline{p}_b & p_9 \\ p_x & p_x \end{bmatrix} \tag{4.17}
$$

$$
\times e^{\pi i \left\{ (h_a - \overline{h}_a) + (h_c - \overline{h}_c) - (h_b - \overline{h}_b) \right\}} \, .
$$

In the final equation, we employ the *s-u* crossing transformation formula (2.20). Repeating the same procedure (except for the use of eq. (2.21) in the final step) to the right half of the link in eq. (4.16) and applying the Wilson bubble formula (2.22) twice and the Wilson triangle identity (2.23) once result in

$$
= \frac{\delta(p_z - p_c)}{\rho_0(p_z) C_{zxx}} \frac{\delta(\overline{p}_z - \overline{p}_c)}{\rho_0(\overline{p}_z) C_{\overline{z}xx}} \frac{\delta(p_z - p_f)}{\rho_0(p_z) C_{zyy}} \frac{\delta(\overline{p}_z - \overline{p}_f)}{\rho_0(\overline{p}_z) C_{\overline{z}yy}}
$$

$$
\times \frac{1}{\rho_0(p) C_{pzw} \rho_0(\overline{p}) C_{\overline{pzw}}} F_{p_9 p} \begin{bmatrix} p_e & p_b \\ p_w & p_z \end{bmatrix} F_{p_9 \overline{p}} \begin{bmatrix} \overline{p}_e & \overline{p}_b \\ \overline{p}_w & \overline{p}_z \end{bmatrix} \, . \tag{4.18}
$$

This equation, combined with the procedure (4.17), enables us to rephrase the state in the integrand in the second line of eq. (4.16) into

$$
= \int_0^\infty dp_a d\overline{p}_a dp_b d\overline{p}_b dp_d d\overline{p}_d p_e d\overline{p}_e \, F_{p_1 p_a} \begin{bmatrix} p_\alpha & p_2 \\ p_x & p_9 \end{bmatrix} F_{p_1 \overline{p}_a} \begin{bmatrix} p_\alpha & p_2 \\ p_x & p_9 \end{bmatrix}
$$

$$
\times F_{p_5 p_d} \begin{bmatrix} p_6 & p_\beta \\ p_9 & p_y \end{bmatrix} F_{p_5 \overline{p}_d} \begin{bmatrix} p_6 & p_\beta \\ p_9 & p_y \end{bmatrix} F_{p_2 p_b} \begin{bmatrix} p_\alpha & p_\alpha \\ p_a & p_x \end{bmatrix} F_{p_2 \overline{p}_b} \begin{bmatrix} p_\alpha & p_\alpha \\ \overline{p}_a & p_x \end{bmatrix} F_{p_6 p_e} \begin{bmatrix} p_\beta & p_\beta \\ p_d & p_y \end{bmatrix} \tag{4.19}
$$

$$
\times F_{p_6 \overline{p}_e} \begin{bmatrix} p_\beta & p_\beta \\ \overline{p}_d & p_y \end{bmatrix} F_{p_a p_z} \begin{bmatrix} p_b & p_9 \\ p_x & p_x \end{bmatrix} F_{\overline{p}_a \overline{p}_z} \begin{bmatrix} \overline{p}_b & p_9 \\ p_x & p_x \end{bmatrix} F_{p_d p_w} \begin{bmatrix} p_e & p_9 \\ p_y & p_y \end{bmatrix} F_{\overline{p}_d \overline{p}_w} \begin{bmatrix} \overline{p}_e & p_9 \\ p_y & p_y \end{bmatrix} F_{p_9 p} \begin{bmatrix} p_e & p_b \\ p_w & p_z \end{bmatrix} F_{p_9 \overline{p}} \begin{bmatrix} \overline{p}_e & \overline{p}_b \\ \overline{p}_w & \overline{p}_z \end{bmatrix}
$$

$$
\times \frac{e^{\pi i \left\{ (h_a - \overline{h}_a) + (h_z - \overline{h}_z) - (h_b - \overline{h}_b) \right\} - \pi i \left\{ (h_d - \overline{h}_d) + (h_w - \overline{h}_w) - (h_e - \overline{h}_e) \right\}}}{\rho_0(p_z) \rho_0(\overline{p}_z) \rho_0(p_w) \rho_0(\overline{p}_w) \rho_0(p) \rho_0(\overline{p}) C_{zxx} C_{\overline{z}xx} C_{wyy} C_{\overline{w}yy} C_{pzw} C_{\overline{pzw}}} \, .
$$

Substituting this equation into eq. (4.16) and performing the integration w.r.t. (i) p_1 and p_5 (ii) p_2 and p_6 in this order in eq. (4.15) with the aid of eq. (A.16) uncomplicates the outer boundary state in a way

$$\left| \left(\vcenter{\hbox{}} \right) \right\rangle = \int_0^\infty dp_9 dp_\alpha dp_\beta \, \rho_0(p_9)\rho_0(p_\alpha)\rho_0(p_\beta) \frac{\delta(p_x - \overline{p}_x)\delta(p_y - \overline{p}_y)}{\rho_0(p_x)\rho_0(p_y)}$$

$$\times \int_0^\infty dp_a dp_b dp_d dp_e \, \rho_0(p_a)\rho_0(p_b)\rho_0(p_d)\rho_0(p_e) C_{x9a} C_{y9d} C_{axb} C_{yde} C_{\alpha\alpha b} C_{\beta\beta e} \qquad (4.20)$$

$$\times F_{p_a p_z}\begin{bmatrix} p_b & p_9 \\ p_x & p_x \end{bmatrix} F_{p_a \overline{p}_z}\begin{bmatrix} p_b & p_9 \\ p_x & p_x \end{bmatrix} F_{p_d p_w}\begin{bmatrix} p_e & p_9 \\ p_y & p_y \end{bmatrix} F_{p_d \overline{p}_w}\begin{bmatrix} p_e & p_9 \\ p_y & p_y \end{bmatrix} F_{p_9 p}\begin{bmatrix} p_e & p_b \\ p_w & p_z \end{bmatrix} F_{p_9 \overline{p}}\begin{bmatrix} p_e & p_b \\ \overline{p}_w & \overline{p}_z \end{bmatrix}$$

$$\times \frac{e^{\pi i \left\{(h_z - \overline{h}_z) - (h_w - \overline{h}_w)\right\}}}{\rho_0(p_z)\rho_0(\overline{p}_z)\rho_0(p_w)\rho_0(\overline{p}_w) C_{zxx} C_{\overline{z}xx} C_{wyy} C_{\overline{w}yy} C_{pzw} C_{\overline{pzw}}} \left| \left(\vcenter{\hbox{}} \right) \right\rangle.$$

We further carry out the integration w.r.t. p_a and p_d, and then p_9 by eq. (A.16) and substitute the result to eq. (4.14) to arrive at the final form

$$\left| \left(\vcenter{\hbox{}} \right) \right\rangle = \frac{\delta(p - \overline{p})}{\rho_0(p)} \int_0^\infty dp_x dp_y dp_z dp_w \, \rho_0(p_x)\rho_0(p_y)\rho_0(p_z)\rho_0(p_w)$$

$$\times C_{xxz} C_{yyw} C_{pzw} \int_0^\infty dp_\alpha dp_\beta dp_b dp_e \, \rho_0(p_\alpha)\rho_0(p_\beta)\rho_0(p_b)\rho_0(p_e)$$

$$\times C_{\alpha\alpha b} C_{\beta\beta e} C_{pbe} \left| \left(\vcenter{\hbox{}} \right) \right\rangle \otimes \left| \left(\vcenter{\hbox{}} \right) \right\rangle$$

$$= \frac{\delta(p - \overline{p})}{\rho_0(p)} \left| \left(\vcenter{\hbox{}} \right) \right\rangle \otimes \left| \left(\vcenter{\hbox{}} \right) \right\rangle. \qquad (4.21)$$

Thus, we conclude that the partition function of the genus two wormhole $\Sigma_{2,0} \times [0,1]$ with the Wilson line $L_p \boxtimes \overline{L}_{\overline{p}}$ connecting the two boundaries actually factorizes after condensating the diagonal condensable anyon (4.1). The generalization to any $\Sigma_{g,n} \times [0,1]$ is conceptually straightforward but practically quite strenuous.

5 Conclusions and discussions

This paper begins with a review of Virasoro TQFT in Section 2, summarizing the structure of the Hilbert space and methods for calculating partition functions using Heegaard splittings and compression bodies. We then shows that, when a solid torus is treated within the framework of VTQFT, conventional results such as the Hawking-Page phase transition and black hole entropy can be derived. Section 3 provides an overview of anyon condensation in non-Abelian TQFT and introduces the concept of diagonal condensable

anyons. In Section 4, we make an attempt to extend the results from Section 3 to VTQFT, showing that the 2-boundary wormholes actually factorize. Let us conclude this paper with comments on the possible future direction.

Mathematical formulation

It is non-trivial to define the concept of a direct sum for continuous labels that appears in the diagonal condensable anyon (4.1). The continuous spectrum also renders the symmetry category less well-behaved, as depicted in Figure 6. A rigorous categorical formulation of VTQFT could deepen our understanding of the TQFT formulation of three-dimensional quantum gravity. The key challenge is that the category associated with VTQFT is neither finite nor semisimple as depicted in the Figure 6 in Appendix B. An intriguing direction for future research is whether the concept of a coend can be formulated for tensor categories that are not finite (Ref. [53] might be useful in this regard).

Other types of condensable anyons and sum over topologies

The diagonal condensable anyon (4.1) is not expected to be the unique condensable anyon in VTQFT. In particular, if we restrict attention to the commutative condition (3.12) for condensable anyons, a similar argument to that in Subsection 3.3 of Ref. [23] shows that for any s and t satisfying $s^2 - t^2 \in \mathbb{Z}$, the direct sum $\bigoplus_{s,t} L_s \boxtimes \overline{L}_t$ is commutative. In Chern-Simons theory, there are multiple ways to choose Lagrangian condensable anyons, and the partition functions for solid tori that result from condensing each of them corresponds to the ADE classification of the Wess-Zumino-Witten model [54, 55]. If such a classification of condensable anyons is completed in VTQFT, it would allow for the discussion of the summation over all possible anyon condensations as mentioned in Ref. [26], which may correspond to bulk side description of the ensemble average of boundary theories. Furthermore, while this paper has demonstrated factorization for a fixed geometry, the full partition function of quantum gravity (1.2) involves a summation over orbits under the action of the mapping class group. It would be interesting to investigate whether factorization persists after summing over topologies.

Relation to topological quantum computing

Chern-Simons theory serves as the low-energy effective theory for the quantum Hall effect and has been shown to be universal as a qubit model [56]. The concept of topological quantum computing [57] was initiated by A. Y. Kitaev, and there has been intensive research on anyon systems such as the Fibonacci anyon, $SU(N)$ Chern-Simons, and topological error-correcting codes like the toric code. In the case of VTQFT, the spectrum is continuously infinite posing the significant challenge of whether such a system can be realized in physical systems. Nevertheless, it remains an interesting question if this system can perform universal quantum computation. Concerning universality, one possible approach, similar to the proof for Fibonacci anyons, involves assigning the $|0\rangle$ and $|1\rangle$ states to a four-point block with four interacting anyons. However, it will cause an excessive number of unnecessary states $|N\rangle$ due to the infinite number of Wilson lines. While the braiding of the first and second anyons only introduces a phase $B_{p_3}^{p_1 p_2}$ in eq. (2.17), the braiding of the second and third anyons leads to a complicated transformation as shown in eq. (2.19). It remains unclear whether this braiding can be expressed in a block-diagonal form. Furthermore, it is highly challenging whether the group generated by these two operations is dense within the set of unitary operation. One possibility is that this system is better suited for use as a general qudit model rather than as a qubit model.

Acknowledgments

A   Crossing kernels and Moore-Seiberg consistency conditions

In this appendix, we collect some crossing equation for Virasoro conformal blocks. Most of the results are excerpted from the review [58]. Although not all of them are used in the main body, we derive a number of practical formulae in detail for the reader's sake of reading original constructions [12, 13] and related literature. For rational conformal field theories (RCFT), the number of primary operators is finite and the crossing transformations like fusion transformation, braiding and modular S-transformation are all expressed as finite size matrices satisfying hexagon identity, pentagon identity among others [37]. However, due to the continuously inifinite number of primaries labeled by $p \in \mathbb{R}_{\geq 0}$ in Liouville theory, the crossing transformations are rather represented as integration kernels whose explicit form was first developed in Refs. [59–61].

Before advancing to tedious consistency equations, here is the easiest case that follows from the four point crossing relation without reference to them:

$$
\begin{array}{c}
\includegraphics
\end{array}
= \int_0^\infty dp\, F_{p3p} \begin{bmatrix} p_3 & p_2 \\ \mathbb{1} & p_1 \end{bmatrix} \qquad . \qquad (A.1)
$$

Recall that $p_4 = \mathbb{1}$ is used to denote $p_4 = \pm i \frac{Q}{2}$. The diagrams on both sides are actually three point blocks, so we find that

$$
F_{p3p} \begin{bmatrix} p_3 & p_2 \\ \mathbb{1} & p_1 \end{bmatrix} = \delta(p_1 - p). \qquad (A.2)
$$

Other crossing transformation with simple analytic expession is the torus modular S-kernel $S_{p_1 p_2}[\mathbb{1}]$ deduced from the precise form of the of the Virasoro characters (2.50) and the

relation $\chi_{p_1}(-\frac{1}{\tau}) = \int_0^\infty dp_2 \, S_{p_1 p_2}[\mathbb{1}]\chi_{p_2}(\tau)$:

$$S_{p_1 p_2}[\mathbb{1}] = 2\sqrt{2}\cos(4\pi p_1 p_2), \tag{A.3}$$

$$S_{\mathbb{1}p}[\mathbb{1}] = 4\sqrt{2}\sinh(2\pi bp)\sinh\left(2\pi\frac{p}{b}\right). \tag{A.4}$$

We now explore the constraints on the general fusion kernel and the general modular S-kernel. The first two indicate that applying F and S twice will return the block to its original state.

Invertiblity of modular S-kernel

$$\int_0^\infty dp_2 \, S_{p_1 p_2}[p_0] S_{p_2 p_3}[p_0] = e^{\pi i h_0}\delta(p_1 - p_3) \tag{A.5}$$

$$\int_0^\infty dp_2 \, S_{p_1 p_2}[p_0] S_{p_2 p_3}^*[p_0] = \delta(p_1 - p_3) \tag{A.6}$$

---

invertibility of fusion kernel

$$\int_0^\infty dp_t \, F_{p_s p_t}\begin{bmatrix} p_3 & p_2 \\ p_4 & p_1 \end{bmatrix} F_{p_t p_u}\begin{bmatrix} p_4 & p_3 \\ p_1 & p_2 \end{bmatrix} = \delta(p_s - p_u) \tag{A.7}$$

The next two are not only highly powerful constraints, but also come with a variety of insightful implications.

Hexagon identity

$$\int_0^\infty dp_t \, e^{\pi i\left(\sum_{i=1}^4 h_i - h_s - h_t - h_u\right)} F_{p_s p_t}\begin{bmatrix} p_3 & p_2 \\ p_4 & p_1 \end{bmatrix} F_{p_t p_u}\begin{bmatrix} p_1 & p_3 \\ p_4 & p_2 \end{bmatrix} = F_{p_s p_u}\begin{bmatrix} p_3 & p_1 \\ p_4 & p_2 \end{bmatrix} \tag{A.8}$$

$$\Longleftrightarrow \int_0^\infty dp_t \, e^{\pi i\left(h_s + h_t + h_u - \sum_{i=1}^4 h_i\right)} F_{p_s p_t}\begin{bmatrix} p_3 & p_2 \\ p_4 & p_1 \end{bmatrix} F_{p_t p_u}\begin{bmatrix} p_1 & p_3 \\ p_4 & p_2 \end{bmatrix} = F_{p_s p_u}\begin{bmatrix} p_3 & p_1 \\ p_4 & p_2 \end{bmatrix} \tag{A.9}$$

From the first to the second line, we multiply both sides by $e^{\pi i h_u} F_{p_u p_a}\begin{bmatrix} p_4 & p_1 \\ p_2 & p_3 \end{bmatrix}$, integrate over p_u and use the identity (A.7), then rewrite the subscript as $u \to t$, $a \to u$ and $1 \leftrightarrow 2$.

Pentagon identity

$$\int_0^\infty dp_t \, F_{p_s p_t}\begin{bmatrix} p_3 & p_2 \\ p_u & p_1 \end{bmatrix} F_{p_u p_v}\begin{bmatrix} p_4 & p_t \\ p_5 & p_1 \end{bmatrix} F_{p_t p_w}\begin{bmatrix} p_4 & p_3 \\ p_v & p_2 \end{bmatrix} = F_{p_s p_v}\begin{bmatrix} p_w & p_2 \\ p_5 & p_1 \end{bmatrix} F_{p_u p_w}\begin{bmatrix} p_4 & p_3 \\ p_5 & p_s \end{bmatrix} \tag{A.10}$$

Readers may wonder if we could obtain a new formula when multiplying both sides by $F_{p_w p_x}\begin{bmatrix} p_v & p_4 \\ p_2 & p_3 \end{bmatrix}$, integrate over p_w and use the identity (A.7) in the same way as the second

eq. (A.9), but it turns out that the result is nothing but eq. (A.10) itself. If we set $p_s = p_3$, $p_u = \mathbb{1}$, $p_4 = p_5$ to apply the formula (A.2), and change subscripts as $1 \to s$, $2 \to 1$, $3 \to 2$, $4 \to 3$, $v \to 4$, $w \to t$, we obtain

Corollary 1: Tetrahedral symmetry of F-symbol

$$F_{\mathbb{1}p_4}\begin{bmatrix} p_3 & p_s \\ p_3 & p_s \end{bmatrix} F_{p_s p_t}\begin{bmatrix} p_3 & p_2 \\ p_4 & p_1 \end{bmatrix} = F_{p_2 p_4}\begin{bmatrix} p_t & p_1 \\ p_3 & p_s \end{bmatrix} F_{\mathbb{1}p_t}\begin{bmatrix} p_3 & p_2 \\ p_3 & p_2 \end{bmatrix} \tag{A.11}$$

A brief reflection with reference to eq. (A.12) uncovers a property of fusion kernel F as follows.

Corollary 2

$$F_{\mathbb{1}p}\begin{bmatrix} p_2 & p_1 \\ p_2 & p_1 \end{bmatrix} = \rho_0(p)C_0(p_1, p_2, p) \tag{A.12}$$

In this identity, $C_0(p_1, p_2, p_3)$ is a certain totally symmetric function and $\rho_0(p)$ is some function in p whose explicit forms are to be determined below. Taking into account the degenerate fusion rule and the shift relation (see Subsection 2.7 in Ref. [58]), it turns out that

$$C_0(p_1, p_2, p_3) = \frac{1}{\sqrt{2}} \frac{\Gamma_b(2Q)}{\Gamma_b(Q)^3} \frac{\Gamma_b\left(\frac{Q}{2} \pm ip_1 \pm ip_2 \pm ip_3\right)}{\prod_{a=1,2,3} \Gamma_b(Q + 2ip_a)\Gamma_b(Q - 2ip_a)}. \tag{A.13}$$

We also see by taking the limit $p_1 \to \mathbb{1}$ in eq. (A.12), combined with eq. (A.2) that

Corollary 3

$$\lim_{p_1 \to \mathbb{1}} C_0(p_1, p_2, p) = \frac{1}{\rho_0(p)}\delta(p - p_2) \tag{A.14}$$

Starting with the invertibility of the fusion kernel F (A.7) and using the tetrahedral symmetry (A.11),

$$\begin{aligned}
\delta(p_s - p_u) &= \int_0^\infty dp_t\, F_{p_s p_t}\begin{bmatrix} p_3 & p_2 \\ p_4 & p_1 \end{bmatrix} F_{p_t p_u}\begin{bmatrix} p_4 & p_3 \\ p_1 & p_2 \end{bmatrix} \\
&= \int_0^\infty dp_t\, \frac{\rho_0(p_t)C_0(p_t, p_2, p_3)}{\rho_0(p_4)C_0(p_4, p_s, p_3)} F_{p_2 p_4}\begin{bmatrix} p_t & p_1 \\ p_3 & p_s \end{bmatrix} F_{p_t p_u}\begin{bmatrix} p_4 & p_3 \\ p_1 & p_2 \end{bmatrix} \\
&= \int_0^\infty dp_t\, \frac{\rho_0(p_t)C_0(p_t, p_2, p_3)}{\rho_0(p_4)C_0(p_4, p_s, p_3)} F_{p_2 p_4}\begin{bmatrix} p_1 & p_t \\ p_s & p_3 \end{bmatrix} F_{p_t p_u}\begin{bmatrix} p_4 & p_3 \\ p_1 & p_2 \end{bmatrix} \\
&= \int_0^\infty dp_t\, \frac{\rho_0(p_t)C_0(p_t, p_2, p_3)\cancel{\rho_0(p_4)}C_0(p_t, p_1, p_4)}{\cancel{\rho_0(p_4)}C_0(p_4, p_s, p_3)\rho_0(p_s)C_0(p_2, p_1, p_s)} F_{p_t p_s}\begin{bmatrix} p_4 & p_3 \\ p_1 & p_2 \end{bmatrix} F_{p_t p_u}\begin{bmatrix} p_4 & p_3 \\ p_1 & p_2 \end{bmatrix}. \tag{A.15}
\end{aligned}$$

We can rearrange this into a version of fusion kernel invertibility formula (A.7):

$$\int_0^\infty dp_t\, \rho_0(p_t) C_0(p_1, p_4, p_t) C_0(p_2, p_3, p_t) F_{p_t p_s} \begin{bmatrix} p_1 & p_2 \\ p_4 & p_3 \end{bmatrix} F_{p_t p_u} \begin{bmatrix} p_1 & p_2 \\ p_4 & p_3 \end{bmatrix}$$

$$= \rho_0(p_s) C_0(p_1, p_2, p_s) C_0(p_3, p_4, p_s) \delta(p_s - p_u) \qquad \text{(A.16)}$$

Given all these ingredients, the shift equation (3.22) in [58] demonstrates that in terms of the Barnes double gamma function $\Gamma_b(z)$ and the double sine function $S_b(z) := \frac{\Gamma_b(z)}{\Gamma_b(Q-z)}$,

$$F_{p_s p_t} \begin{bmatrix} p_1 & p_2 \\ p_3 & p_4 \end{bmatrix} = \frac{\Gamma_b(Q \pm 2ip_s)}{\Gamma_b(2ip_t)} \frac{\Gamma_b(\frac{Q}{2} \pm ip_t - ip_3 \pm ip_4) \Gamma_b(\frac{Q}{2} \pm ip_t + ip_1 \pm ip_2)}{\Gamma_b(\frac{Q}{2} \pm ip_s \pm ip_2 - ip_3) \Gamma_b(\frac{Q}{2} \pm ip_s + ip_1 \pm ip_4)}$$

$$\times (-i) \int_{\frac{Q}{4} + i\mathbb{R}} dz\, \frac{S_b(z + (ip_1 \pm ip_4)) S_b(z + (\pm ip_2 - ip_3))}{S_b(z + (\frac{Q}{2} \pm ip_t + ip_1 - ip_3)) S_b(z + (\frac{Q}{2} \pm ip_s))}. \qquad \text{(A.17)}$$

It is worth noting that $F_{p_s p_t}$ is real for $p_1, \cdots, p_4, p_s, p_t \in \mathbb{R}_{\geq 0}$.

Lastly, we now move on to introduce the other consistency equation to determine $S_{p_1 p_2}[p_0]$. The equation involves all three basic crossing moves on a 2-punctured torus.

$$S_{p_1 p_2}[p_3] \int_0^\infty dp_4\, F_{p_3 p_4} \begin{bmatrix} p_2 & p_0 \\ p_2 & p_0 \end{bmatrix} e^{2\pi i(h_4 - h_2)} F_{p_4 p_5} \begin{bmatrix} p_0 & p_0 \\ p_2 & p_2 \end{bmatrix}$$

$$= \int_0^\infty dp_6\, F_{p_3 p_6} \begin{bmatrix} p_1 & p_0 \\ p_1 & p_0 \end{bmatrix} F_{p_1 p_5} \begin{bmatrix} p_0 & p_0 \\ p_6 & p_6 \end{bmatrix} e^{\pi i(2h_0 - h_5)} S_{p_6 p_2}[p_5] \qquad \text{(A.18)}$$

If we take the limit $p_3 \to i\frac{Q}{2}$, $p_1 \to i\frac{Q}{2}$ in this order, the first fusion kernel F in the integrand of the second line converges to the limit

$$\lim_{p_1 \to i\frac{Q}{2}} \lim_{p_3 \to i\frac{Q}{2}} F_{p_3 p_6} \begin{bmatrix} p_1 & p_0 \\ p_1 & p_0 \end{bmatrix} = \lim_{p_1 \to i\frac{Q}{2}} \rho_0(p_6) C_0(p_0, p_1, p_6) = \delta(p_0 - p_6), \qquad \text{(A.19)}$$

which reduces eq. (A.18) to

$$S_{\mathbb{1} p_2}[\mathbb{1}] \int_0^\infty dp_4\, F_{\mathbb{1} p_4} \begin{bmatrix} p_2 & p_0 \\ p_2 & p_0 \end{bmatrix} e^{2\pi i(h_4 - h_2)} F_{p_4 p_5} \begin{bmatrix} p_0 & p_0 \\ p_2 & p_2 \end{bmatrix} = F_{\mathbb{1} p_5} \begin{bmatrix} p_0 & p_0 \\ p_0 & p_0 \end{bmatrix} e^{\pi i(2h_0 - h_5)} S_{p_0 p_2}[p_5].$$

$$\text{(A.20)}$$

After renaming $1 \to 2$, $5 \to 0$ and $4 \to a$, we obtain

$$S_{p_1 p_2}[p_0] = S_{\mathbb{1} p_2}[\mathbb{1}] \int_0^\infty dp_a\, \frac{\rho_0(p_a) C_0(p_1, p_2, p_a)}{\rho_0(p_0) C_0(p_1, p_1, p_0)} e^{\pi i(2h_a - 2h_2 - 2h_1 + h_0)} F_{p_a p_0} \begin{bmatrix} p_1 & p_1 \\ p_2 & p_2 \end{bmatrix} \quad \text{(A.21)}$$

$$= \int_0^\infty dp_a\, \frac{\rho_0(p_2) C_0(p_0, p_2, p_2)}{C_0(p_a, p_1, p_2)} e^{\pi i(2h_a - 2h_2 - 2h_1 + h_0)} F_{p_0 p_a} \begin{bmatrix} p_2 & p_1 \\ p_2 & p_1 \end{bmatrix} \qquad \text{(A.22)}$$

This corollary states that the modular S-kernel is fully determined by the fusion kernel F, so in order to tell the exact form of them it suffice to compute F, which is already obtained in eq. (A.17). We also see from the first identity that the r. h. s. of

$$\frac{S_{p_1p_2}[p_0]}{S_{\mathbb{1}p_2}[\mathbb{1}]}C_0(p_1,p_1,p_0) = \int_0^\infty dp_a \frac{\rho_0(p_a)C_0(p_1,p_2,p_a)}{\rho_0(p_0)}e^{\pi i(2h_a-2h_2-2h_1+h_0)}F_{p_ap_0}\begin{bmatrix}p_1 & p_1 \\ p_2 & p_2\end{bmatrix},$$
(A.23)

is symmetric under $p_1 \leftrightarrow p_2$, leading to the following result:

Corollary 6: Symmetric property of S-kernel

$$\frac{S_{p_1p_2}[p_0]}{S_{\mathbb{1}p_2}[\mathbb{1}]}C_0(p_1,p_1,p_0) = \frac{S_{p_2p_1}[p_0]}{S_{\mathbb{1}p_1}[\mathbb{1}]}C_0(p_2,p_2,p_0) \tag{A.24}$$

Taking the limit $p_0 \to \mathbb{1}$ and using the property (A.14) lead to the equality

---

Corollary 7

$$\rho_0(p) = S_{\mathbb{1}p}[\mathbb{1}] = 4\sqrt{2}\sinh(2\pi bp)\sinh\left(2\pi\frac{p}{b}\right) \tag{A.25}$$

The relation between modular S-kernel and fusion kernel (A.21), along with eq. (A.17) leads to the precise form

$$S_{p_1p_2}[p_0] = S_b\left(\frac{Q}{2}-p_0\right)\rho_0(p_2)\frac{\Gamma_b(Q \pm 2p_1)\Gamma_b\left(\frac{Q}{2}-p_0 \pm 2p_2\right)}{\Gamma_b(Q \pm 2p_2)\Gamma_b\left(\frac{Q}{2}+p_0 \pm 2p_1\right)}$$

$$\times e^{\frac{\pi i}{2}\left(-p_0Q-2p_0^2\right)+2\pi i\left(p_1^2+p_2^2\right)} \cdot \frac{1}{2i}\int_0^\infty dp\, e^{-2\pi ip^2}\frac{S_b\left(\frac{Q}{4}+\frac{p_0}{2} \pm p_1 \pm p_2 \pm p\right)}{S_b(\pm 2p)}. \tag{A.26}$$

By this identity it also holds that $S_{p_1p_2}^*[p_0] = e^{-\pi i h_0}S_{p_1p_2}[p_0]$ in accordance with eqs. (A.5), (A.6).

B From monoidal category to fusion category and modular tensor category

In lower-dimensional TQFT, the mathematics of primary importance includes category theory, particularly fusion categories and modular tensor categories, both of which are grounded in the theory of tensor categories. A tensor category is a specific version of a more fundamental structure, a monoidal category that is a category with a product structure (*tensor product*) and a special object (*unit object*). Although the terms "monoidal category" and "tensor catogory" are sometimes used interchangeably, we treat them as distinct concepts in accordance with the polished textbook [51]. The rigorous construction from monoidal categories to fusion categories and modular tensor categories through tensor categories is exquisitely explored in Refs. [45, 51]. However, the construction is fairly lengthy due to the need for a number of interweaving definitions such as "braided", "locally finite", "sovereign" and others, which may introduce unnecesarry complexities when
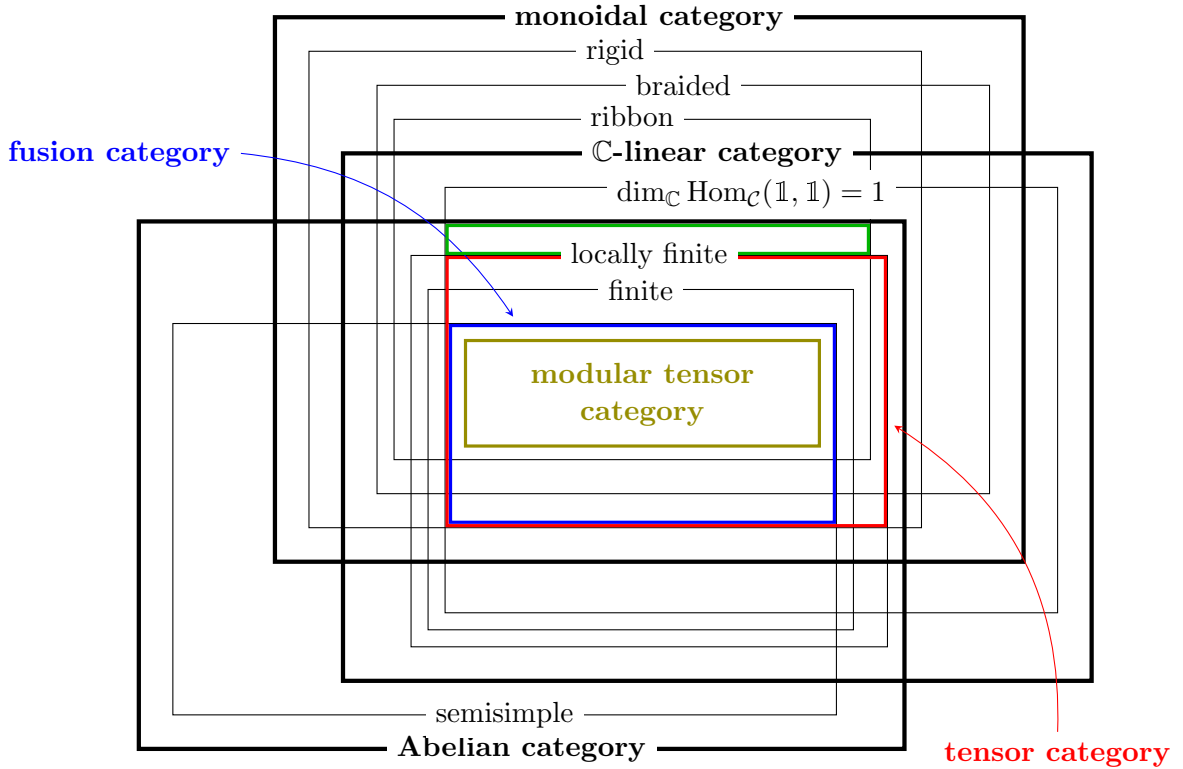
Figure 6. Inclusion relation for various categorical definitions. Surrounded by the red rectangle is the family of tensor categories. The fusion categories are marked inside the blue rectangle and categories in the olive region satisfying the modularity condition are MTC. The green region is where the symmetry category of VTQFT is located. All the colored regions are inside the intersection of (i) monoidal categories (ii) Abelian categories (iii) $\mathbb{C}$-linear categories.

interpreting physical implications. Here we elucidate their relations rather than to just itemize the cluster of precise definitions.

Let us examine the categorical concepts that constitute fusion categories and modular tensor categories (MTC). 2d TQFTs are characterized by fusion categories, while 3d TQFTs are by MTC . There are three significant classes of fundamental categories needed to formulate tensor categories (see Definition 4.1.1 of [51]), namely (i) monoidal category (ii) Abelian category (iii) $\mathbb{C}$-linear category depicted by bold rectangles in Figure 6.

Monoidal category

> Definition B.1: Monoidal category
>
> A **_monoidal category_** $\mathcal{C}$ is a category $\mathcal{C}$ endowed with the following data:
>
> - A bifunctor $\otimes : \mathcal{C} \times \mathcal{C} \to \mathcal{C}$ called the **_tensor product_**
>
> - A natural isomorphism α called the **_associator_** inducing an isomorphism $\alpha_{X,Y,Z} : (X \otimes Y) \otimes Z \xrightarrow{\sim} X \otimes (Y \otimes Z)$ for all $X, Y, Z \in \mathrm{Obj}\,\mathcal{C}$
>
> - An object $\mathbb{1} \in \mathrm{Obj}\,\mathcal{C}$ called the **_unit_**

satisfying the **pentagon identity** and the **unit axiom** (see Definition 2.1.1 of [51] for details).

The central idea is the existence of a tensor product corresponding to particle fusion and the unit corresponding to the identity line. Two specific classes of monoidal categories capture physically relevant structure in TQFT.

Definition B.2: Rigid category

A **rigid category** is a monoidal category where every object has left and right duals (see Definition 2.10.11 of [51] for details).

In most physical examples, the "dual" of an object is the object itself, so the "left" and "right" is unimportant.

Definition B.3: Braided monoidal category

A **braided monoidal category** is a monoidal category equipped with a natural transformation $R_{X,Y} : X \otimes Y \xrightarrow{\sim} Y \otimes X$ called **braiding** satisfying the **hexagon identity** (see Definition 8.1.1 of [51] for details).

Abelian category

Definition B.4: Additive category

An additive category $\mathcal{C}$ is a category abiding by the conditions

1. $\mathrm{Hom}_{\mathcal{C}}(X, Y)$ is an abelian group for all $X, Y \in \mathrm{Obj}\,\mathcal{C}$.

2. There exists an object 0 called the **zero** such that $\mathrm{Hom}_{\mathcal{C}}(0, 0) = 0$

3. There exists a bifunctor $\oplus : \mathcal{C} \times \mathcal{C} \to \mathcal{C}$ satisfying additional conditions (see Definition 1.2.1 of [51] for details).

The existence of direct sum is of primary importance since it corresponds to particle superposition. An **Abelian category** is an additive category with well-defined notion of kernel ker and image im. We omit the detals since they are not vital in physics (see Definition 1.3.1 of [51]).

Definition B.5: Semisimple category

An additive category $\mathcal{C}$ is semisimple if every $X \in \mathrm{Obj}\,\mathcal{C}$ is a direct sum of simple objects (see Definition 1.5.1 of [51]).

VTQFT does not satisfy the assumption in this definition when it comes to a continuous superposition of Wilson lines. Semisimplicity is essential for formulating the direct sum in a mathematically rigorous manner.

$\mathbb{C}$-linear category

> **Definition B.6: $\mathbb{C}$-linear category**
>
> A $\mathbb{C}$-**linear category** is a $\mathbf{Vect}_{\mathbb{C}}$-enriched category, that is, a category where $\mathrm{Hom}_{\mathcal{C}}(X, Y)$ is a $\mathbb{C}$-vector space for all $X, Y \in \mathrm{Obj}\,\mathcal{C}$.

If $\mathcal{C}$ is additionally an Abelian category, the condition $\dim_{\mathbb{C}} \mathrm{Hom}_{\mathcal{C}}(\mathbb{1}, \mathbb{1}) = 1$ is equivalent to say that $\mathbb{1}$ is a simple object in $\mathcal{C}$.

There are other definitions shown in Figure 6, say **local finiteness** (Definition 1.8.1) and **finiteness** (Definition 1.8.5). Readers may refer to the indicated definition number in [51]. A **tensor category** is a locally finite $\mathbb{C}$-linear Abelian rigid monoidal category with $\dim \mathrm{Hom}_{\mathcal{C}}(\mathbb{1}, \mathbb{1}) = 1$, displayed by the red rectangle in Figure 6. A **fusion category** is a finite semisimple tensor category presented by the blue rectangle. A modular tensor category is a ribbon fusion category with an additional condition (modularity condition, see Definition A.12 in Ref. [45]) shown by the olive rectangle.

References

[1] A. Achucarro and P. K. Townsend, *A Chern-Simons Action for Three-Dimensional anti-De Sitter Supergravity Theories*, Phys. Lett. B **180** (1986) 89.

[2] E. Witten, *Quantum Field Theory and the Jones Polynomial*, Commun. Math. Phys. **121** (1989) 351–399.

[3] E. Witten, *(2+1)-Dimensional Gravity as an Exactly Soluble System*, Nucl. Phys. B **311** (1988) 46.

[4] H. L. Verlinde, *Conformal Field Theory, Two-Dimensional Quantum Gravity and Quantization of Teichmüller Space*, Nucl. Phys. B **337** (1990) 652–680.

[5] J. Teschner, *Quantum Liouville Theory Versus Quantized Teichmüller Spaces*, Fortsch. Phys. **51** (2003) 865–872, [hep-th/0212243].

[6] J. Teschner, *From Liouville Theory to the Quantum Geometry of Riemann Surfaces*, in 14th International Congress on Mathematical Physics, 8, 2003. hep-th/0308031.

[7] J. Teschner, *On the Relation Between Quantum Liouville Theory and the Quantized Teichmüller Spaces*, Int. J. Mod. Phys. A **19S2** (2004) 459–477, [hep-th/0303149].

[8] J. Teschner, *An Analog of a Modular Functor from Quantized Teichmüller Theory*, math/0510174.

[9] R. M. Kashaev, *Quantization of Teichmüller Spaces and the Quantum Dilogarithm*, Letters in Mathematical Physics **43** (1998) 105–115, [q-alg/9705021].

[10] J. E. Andersen and R. Kashaev, *A New Formulation of the Teichmüller TQFT*, arXiv:1305.4291.

[11] V. Mikhaylov, *Teichmüller TQFT vs. Chern-Simons theory*, JHEP **04** (2018) 085, [arXiv:1710.04354].

[12] S. Collier, L. Eberhardt, and M. Zhang, *Solving 3d Gravity with Virasoro TQFT*, SciPost Phys. **15** (2023), no. 4 151, [arXiv:2304.13650].

[13] S. Collier, L. Eberhardt, and M. Zhang, *3d Gravity from Virasoro TQFT: Holography, Wormholes and Knots*, arXiv:2401.13900.

[14] A. Maloney and E. Witten, *Quantum Gravity Partition Functions in Three Dimensions*, JHEP **02** (2010) 029, [arXiv:0712.0155].

[15] J. Cotler and K. Jensen, *AdS$_3$ Gravity and Random CFT*, JHEP **04** (2021) 033, [arXiv:2006.08648].

[16] J. Chandra, S. Collier, T. Hartman, and A. Maloney, *Semiclassical 3D Gravity as an Average of Large-c CFTs*, JHEP **12** (2022) 069, [arXiv:2203.06511].

[17] A. Belin, J. de Boer, D. L. Jafferis, P. Nayak, and J. Sonner, *Approximate CFTs and Random Tensor Models*, JHEP **09** (2024) 163, [arXiv:2308.03829].

[18] D. L. Jafferis, L. Rozenberg, and G. Wong, *3d Gravity as a Random Ensemble*, arXiv:2407.02649.

[19] P. Pelliconi, J. Sonner, and H. Verlinde, *Gravity as a Mesoscopic System*, arXiv:2409.13808.

[20] D. Gaiotto, A. Kapustin, N. Seiberg, and B. Willett, *Generalized Global Symmetries*, JHEP **02** (2015) 172, [arXiv:1412.5148].

[21] L. Bhardwaj and Y. Tachikawa, *On Finite Symmetries and Their Gauging in Two Dimensions*, JHEP **03** (2018) 189, [arXiv:1704.02330].

[22] C.-M. Chang, Y.-H. Lin, S.-H. Shao, Y. Wang, and X. Yin, *Topological Defect Lines and Renormalization Group Flows in Two Dimensions*, JHEP **01** (2019) 026, [arXiv:1802.04445].

[23] F. Benini, C. Copetti, and L. Di Pietro, *Factorization and Global Symmetries in Holography*, SciPost Phys. **14** (2023), no. 2 019, [arXiv:2203.09537].

[24] D. Harlow and H. Ooguri, *Constraints on Symmetries from Holography*, Phys. Rev. Lett. **122** (2019), no. 19 191601, [arXiv:1810.05337].

[25] D. Harlow and H. Ooguri, *Symmetries in Quantum Field Theory and Quantum Gravity*, Commun. Math. Phys. **383** (2021), no. 3 1669–1804, [arXiv:1810.05338].

[26] A. Dymarsky and A. Shapere, *Bulk Derivation of TQFT Gravity*, arXiv:2405.20366.

[27] L. W. Tu, Differential Geometry: Connections, Curvature, and Characteristic Classes, vol. 275. Springer, 2017.

[28] B. Petri, *Introduction to Teichmüller Theory: Lecture Notes*, . https://webusers.imj-prg.fr/~bram.petri/t_tt/notes_240212.pdf.

[29] M. F. Atiyah and R. Bott, *The Yang-Mills Equations over Riemann Surfaces*, Philosophical Transactions of the Royal Society of London. Series A, Mathematical and Physical Sciences **308** (1983), no. 1505 523–615.

[30] C. Scarinci and K. Krasnov, *The Universal Phase Space of AdS$_3$ Gravity*, Commun. Math. Phys. **322** (2013) 167–205, [arXiv:1111.6507].

[31] A. Bhattacharyya, S. Ghosh, P. Nandi, and S. Pal, *3D $\mathcal{N} = 1$ Supergravity from Virasoro TQFT: Gravitational Partition Function and Out-of-Time-Order Correlator*, arXiv:2408.01538.

[32] S. Collier, A. Maloney, H. Maxfield, and I. Tsiares, *Universal Dynamics of Heavy Operators in CFT$_2$*, JHEP **07** (2020) 074, [arXiv:1912.00222].

[33] H. Dorn and H. J. Otto, *Two and Three Point Functions in Liouville Theory*, Nucl. Phys. B **429** (1994) 375–388, [hep-th/9403141].

[34] A. B. Zamolodchikov and A. B. Zamolodchikov, *Structure Constants and Conformal Bootstrap in Liouville Field Theory*, Nucl. Phys. B **477** (1996) 577–605, [hep-th/9506136].

[35] S. Ribault, *Conformal Field Theory on the Plane*, arXiv:1406.4290.

[36] S. Ribault, *Exactly Solvable Conformal Field Theories*, arXiv:2411.17262.

[37] G. W. Moore and N. Seiberg, *Classical and Quantum Conformal Field Theory*, Commun. Math. Phys. **123** (1989) 177.

[38] B. Post and I. Tsiares, *A Non-rational Verlinde Formula from Virasoro TQFT*, arXiv:2411.07285.

[39] J. de Boer, D. Liska, and B. Post, *Multiboundary Wormholes and OPE Statistics*, JHEP **10** (2024) 207, [arXiv:2405.13111].

[40] M. Bañados, C. Teitelboim, and J. Zanelli, *The Black Hole in Three Dimensional Spacetime*, Phys. Rev. Lett. **69** (1992) 1849–1851, [hep-th/9204099].

[41] S. Carlip and C. Teitelboim, *Aspects of Black Hole Quantum Mechanics and Thermodynamics in $(2+1)$-Dimensions*, Phys. Rev. D **51** (1995) 622–631, [gr-qc/9405070].

[42] S. W. Hawking and D. N. Page, *Thermodynamics of Black Holes in anti-De Sitter Space*, Commun. Math. Phys. **87** (1983) 577.

[43] Y. Kurita, *CFT Description of Three-Dimensional Hawking-Page Phase Transition*, . https://www2.yukawa.kyoto-u.ac.jp/~masashi.hamanaka/kurita_y04.pdf.

[44] T. G. Mertens, J. Simón, and G. Wong, *A Proposal for 3d Quantum Gravity and Its Bulk Factorization*, JHEP **06** (2023) 134, [arXiv:2210.14196].

[45] L. Kong, *Anyon Condensation and Tensor Categories*, Nucl. Phys. B **886** (2014) 436–482, [arXiv:1307.8244].

[46] L. Bhardwaj, L. E. Bottini, L. Fraser-Taliente, L. Gladden, D. S. W. Gould, A. Platschorre, and H. Tillim, *Lectures on Generalized Symmetries*, Phys. Rept. **1051** (2024) 1–87, [arXiv:2307.07547].

[47] J. Kaidi, Z. Komargodski, K. Ohmori, S. Seifnashri, and S.-H. Shao, *Higher Central Charges and Topological Boundaries in 2+1-Dimensional TQFTs*, SciPost Phys. **13** (2022), no. 3 067, [arXiv:2107.13091].

[48] K. Roumpedakis, S. Seifnashri, and S.-H. Shao, *Higher Gauging and Non-invertible Condensation Defects*, Commun. Math. Phys. **401** (2023), no. 3 3043–3107, [arXiv:2204.02407].

[49] C. Córdova and D. García-Sepúlveda, *Non-Invertible Anyon Condensation and Level-Rank Dualities*, arXiv:2312.16317.

[50] C. Córdova and D. García-Sepúlveda, *Topological Cosets via Anyon Condensation and Applications to Gapped* **QCD₂**, arXiv:2412.01877.

[51] P. Etingof, S. Gelaki, D. Nikshych, and V. Ostrik, Tensor Categories, vol. 205. American Mathematical Soc. Am. Math. Soc., 2015.

[52] J. Fuchs, I. Runkel, and C. Schweigert, *TFT Construction of RCFT Correlators I. Partition Functions*, Nucl. Phys. B **646** (2002) 353–497, [hep-th/0204148].

[53] L. Chang, Q. T. Kolt, Z. Wang, and Q. Zhang, *Modular Data of Non-semisimple Modular Categories*, arXiv:2404.09314.

[54] A. Cappelli, C. Itzykson, and J. B. Zuber, *Modular Invariant Partition Functions in Two Dimensions*, Nucl. Phys. B **280** (1987) 445–465.

[55] A. Cappelli, C. Itzykson, and J. B. Zuber, *The A-D-E Classification of Minimal and $A_1^{(1)}$ Conformal Invariant Theories*, Commun. Math. Phys. **113** (1987) 1.

[56] M. H. Freedman, M. Larsen, and Z. Wang, *A Modular Functor Which is Universal for Quantum Computation*, Commun. Math. Phys. **227** (2002), no. 3 605–622, [quant-ph/0001108].

[57] A. Y. Kitaev, *Fault Tolerant Quantum Computation by Anyons*, Annals Phys. **303** (2003) 2–30, [`quant-ph/9707021`].

[58] L. Eberhardt, *Notes on Crossing Transformations of Virasoro Conformal Blocks*, `arXiv:2309.11540`.

[59] B. Ponsot and J. Teschner, *Liouville Bootstrap via Harmonic Analysis on a Noncompact Quantum Group*, `hep-th/9911110`.

[60] B. Ponsot and J. Teschner, *Clebsch-Gordan and Racah-Wigner Coefficients for a Continuous Series of Representations of* $\mathcal{U}_q(\mathfrak{sl}(2,\mathbb{R}))$, Commun. Math. Phys. **224** (2001) 613–655, [`math/0007097`].

[61] J. Teschner and G. S. Vartanov, *Supersymmetric Gauge Theories, Quantization of* $\mathcal{M}_{\text{flat}}$, *and Conformal Field Theory*, Adv. Theor. Math. Phys. **19** (2015) 1–135, [`arXiv:1302.3778`].